Chapter 4

Material selected for testing

In this chapter, the soil materials used for testing are described. The methods selected to determine index properties of the tested materials such as grain size distribution, grain shape and size, mineralogy, maximum and minimum void ratio are briefly explained.

4.1 Origin

Four types of materials were used. The host sand consists of a blend of two types of sand. Coarse quartzic sand from the river Maas was mixed with artificially (crushed) quartz sand produced by Sibelco (Belgium) LM25 in a proportion of 2 to 1. In the first series of tests (serie A), the filler material was a quartz flour also produced by Sibelco by iron-free grinding of selected quartz sand with a high silica-content in ball- or vibration mills and control of particle size The flour

Commercialized under the name of M10 was used. In the second series of tests, fines were sampled above a sand quarry in Bierbeek nearby Leuven, Belgium. The Belgium silt belongs to an Eocene loess deposit (see Appendix A) that lies above the sand of Brussels formation.

4.2 Mineralogy

The mineral compositions of the tested materials are shown in the table 4.1. They were determined by X-ray diffraction method. As it can be observed from the table 4-1 the artificial flour is mainly composed of quartz while the Belgium silt also contains mica (9.5 %), feldspar (6.8%) and other minerals (12%), including other clays such as kaolinite and chlorite. t is expected that mica influence the properties of the mixtures made with the Belgium silt. Due to their platy structure and their flexibility.

In this report, the mixtures made with the artificially crushed quartzic silt and with the Belgian silt are named mixtures A and B, respectively.

Table 4- 1 Mineralogy of material used

Names	Percentages			
	Maas sand	Artificial sand	Artificial flour/silt	Belgium silt
Feldspar		-		6.78
Quartz	99	99	99	68.76
Mica		-		9,5
Amphibole		-		0,28
Calcite		-		2,68
Others		1	1	12

4.3 Particle size and shape analysis

To get detailed information about the shape and roughness of the materials tested a high resolution Leica 3D Stereo Explorer used. A small amount of soil was taken as representative of the whole sample for microscopic analysis. Fig 4.1 to 4.3 are photographs of the host sands mixed together, the artificial quartzic sand, the artificial flour and the Belgium silt, respectively.

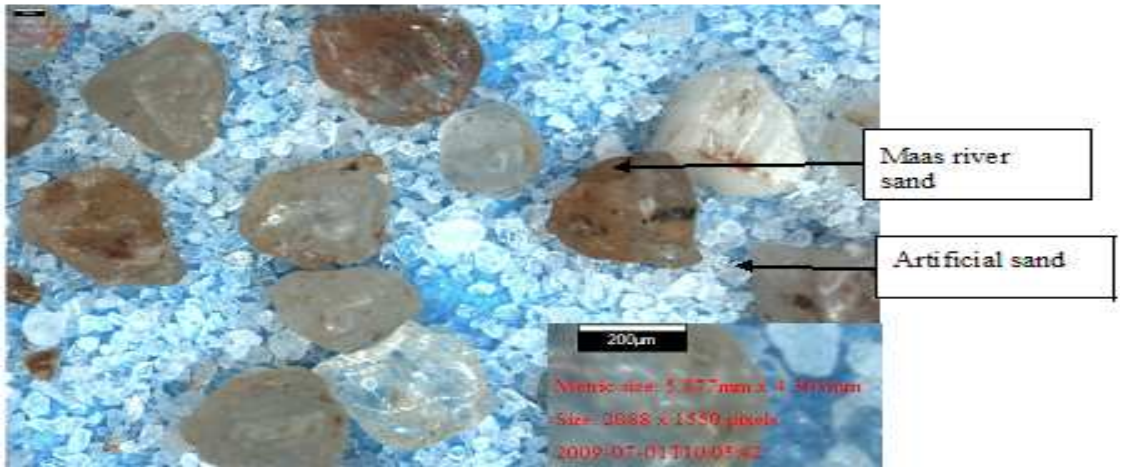

Fig 4. 1 Photograph of the host sand mixtures

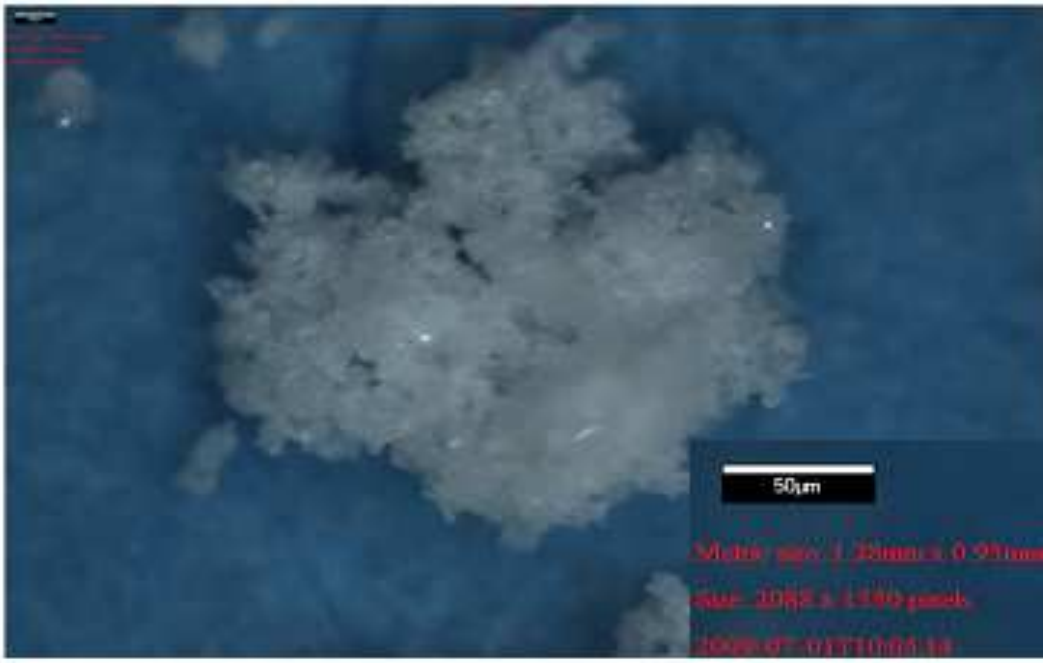

Fig 4. 2 Photograph of artificial silt

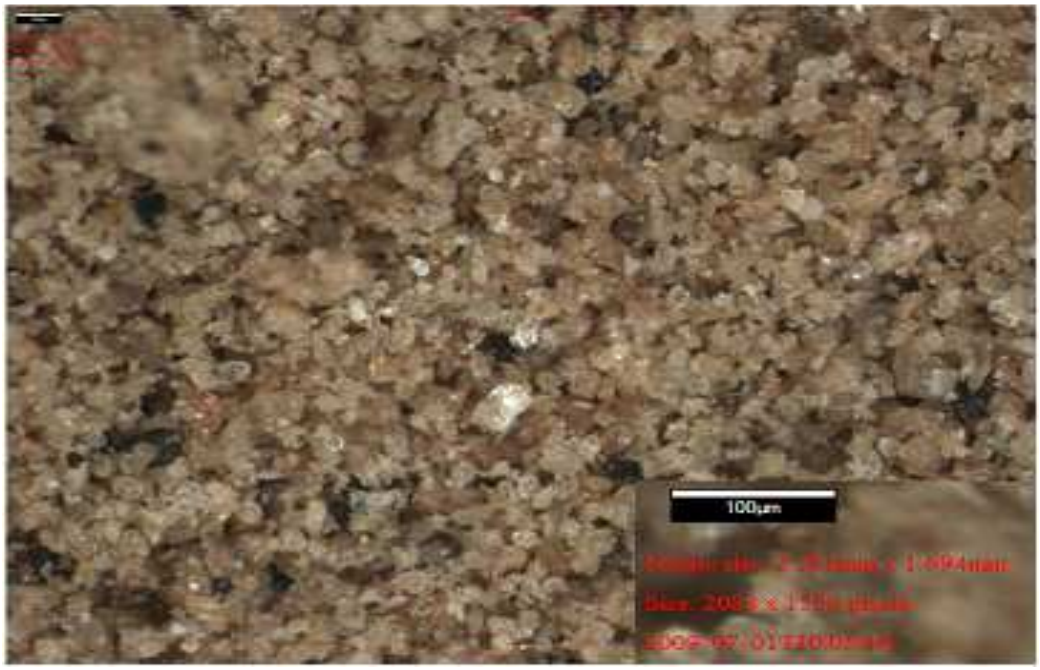

Fig 4. 3 Photograph of Belgium silt

Particles can be described in terms of:

- form, i.e., sphericity, equidimensionality, flatness, elongation),
- angularity using adjectives such as angular, subangular, subround and round to describe the smoothness or sharpness of the particle edges
- Surface texture using adjectives such as smooth, rough, glassy, honeycombed, pitted, striated) to describe the small scale roughness of the grains.

Figures 4.1 show that the coarse sand is spherical and angular to sub-rounded, while the fine sand is non equidimentional and angular as expected for a crushed sand. The surface of the coarse quartz sand grains is clean or stained by iron oxide; it looks smooth and glassy while the surface of the fine sand grains is clean and glassy.

The artificial flour is so fine that its particles cannot be distinguished on photographs taken with a magnification of 50 µm. A Scanning Electronic Microscope (SEM) image provided by Sibelco on its website (see Fig. 4.4) shows that its grains are, as expected, non equidimentional and angular.

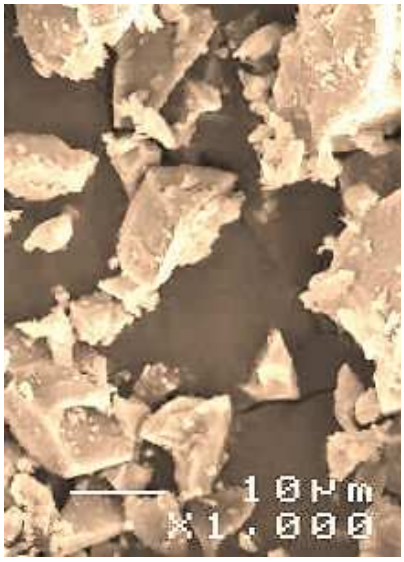

Fig 4. 4 SEM photo of the quartz flour

Belgium silt is not fine that its particles can be distinguished on photographs taken with a magnification of 50 µm. Figure 4.5 shows that its grains are non equidimentional and sub rounded.

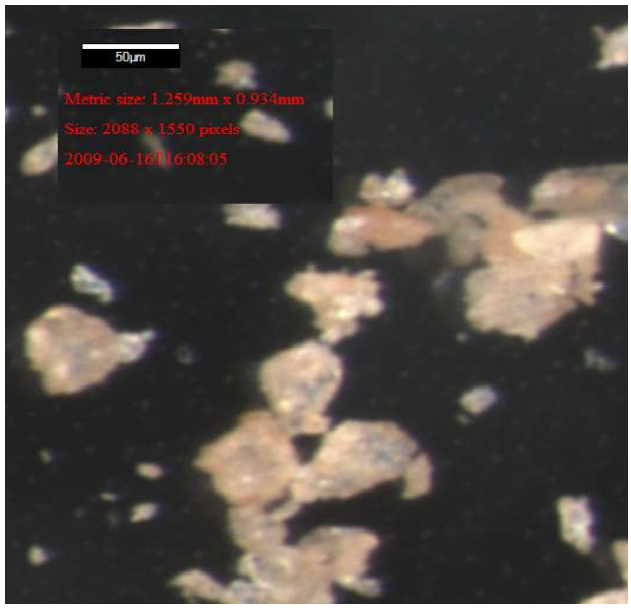

Fig 4. 5 Photo of Belgium silt

4.4 Grain size distribution

The grain size distribution of the coarse and fine sands was established by dry sieving. That of the Belgium silt was determined using wet sieving (BS 1377 part 2:1990:3) and hydrometer sedimentation test (BS 1377: part 2: 1990:9.5). Wet sieving and hydrometer tests were done separately. For the quartz flour consisting of silt only, hydrometer testing was performed.

Results are shown in fig 4.6 and characteristics of grain size parameters are listed in table 4.2. The coarse and fine sands are uniform sands. Their mixture is gap-graded between 0.01 to 1.25 mm and 0.03 to 1.25 mm respectively. Both the quartz flour and the Belgium silt contain a significant percentage of clay size grains (10% and 20% respectively). The coefficient of uniformity of mixtures can be seen from table 4-2 and table 4-3. For artificial silt mixtures the coefficient of uniformity varies from 1,21 to 340 and for Belgium silt mixtures the coefficient of uniformity varies from 1,21 to 157,41.

The sand and silt mixtures were made of host sands and filler materials by mass percentage in order to obtain gap graded soils (fig 4.7).

When preparing the mixtures B, the 2% grains of sand size originating from the Belgian silt were counted as silt.

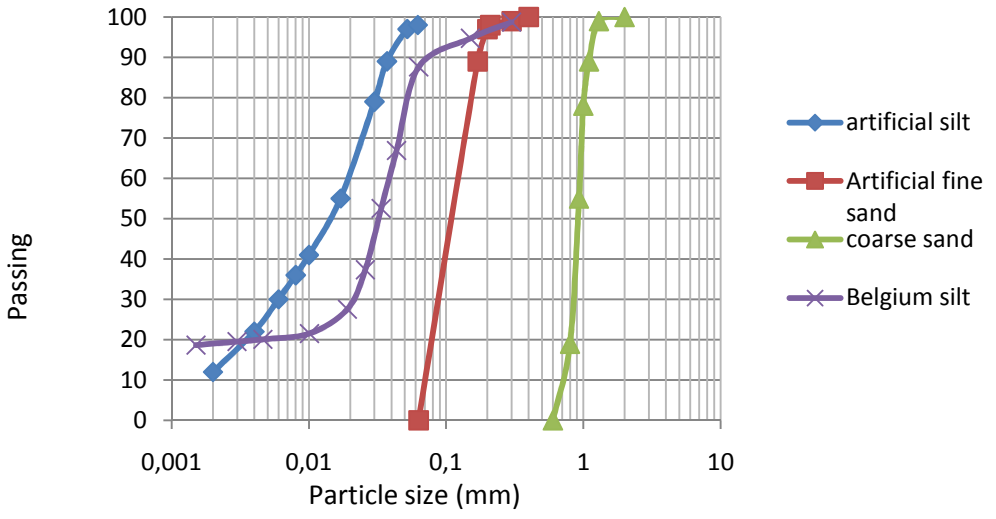

Fig 4. 6 Grain size distributions of tested materials

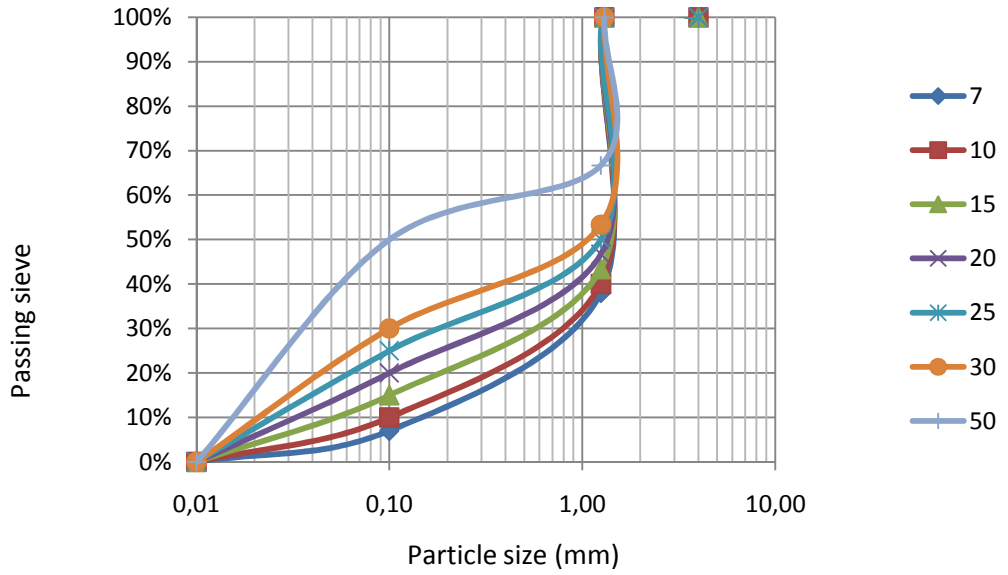

a) Grain size distribution of A mixtures

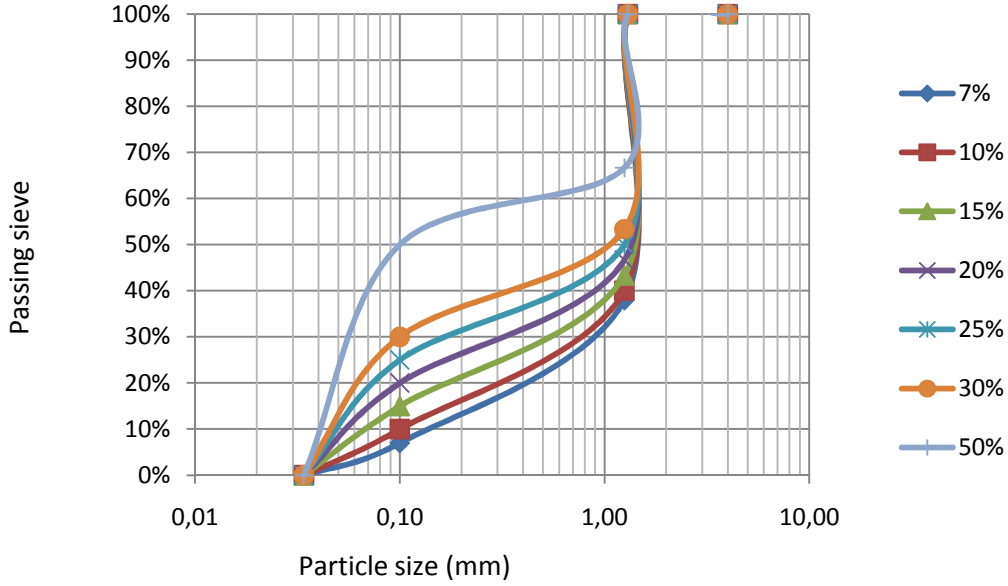

b) Grain size distribution of B mixtures

Fig 4. 7 Grain size distributions of mixtures.

Table 4- 2 Characteristic grain sizes of the A mixtures

Material Fines content,%	Specific gravity g/cm^3	Coefficient of uniformity	D10 mm	D30 mm	D50 Mm
Host sand	2.65	1,21	0,75	0,85	0,9
7	2.67	100,00	0,018	0,7	1,23
10	2.67	175,00	0,01	0,5	1,22
15	2.67	269,23	0,0065	0,25	1,21
20	2.67	309,09	0,0055	0,08	1,2
25	2.67	340,00	0,005	0,025	1,2
30	2.67	326,53	0,0049	0,01	0,9
50	2.67	111,11	0,0045	0,005	0,01
Host silt	2.67	10,00	0,002	0,006	0,0105

Table 4- 3 Characteristic grain sizes of the B mixtures

Material Fines content,%	Specific gravity, g/cm^3	Coefficient of uniformity	D10 mm	D30 mm	D50 mm
Host sand	2.65	1,21	0,75	0,85	0,9
7	2.67	16,67	0,108	1	1,23
10	2.67	17,50	0,1	0,8	1,22
15	2.67	116,67	0,015	0,6	1,21
20	2.67	154,55	0,011	0,35	1,2
25	2.67	157,41	0,0108	0,2	1,2
30	2.67	158,42	0,0101	0,1	0,9
50	2.67	71,43	0,007	0,025	0,1
Host silt	2.67	6,67	0,006	0,02	0,032

4.5 Atterberg limits

Atterberg limits were measured for the Belgium silt only because the Belgium silt is the only cohesive soil among tested host and filler materials. The liquid limit was determined using Casangrande method (BS 1377:1990:4.5). The plastic limit was obtained using British standards (BS 1377:1990:5.2). Belgium silt has a plasticity index of 7% and a liquid limit of 32 %. It plots in the Atterberg chart just below the A-line and left of the 35% liquid limit line. Accordingly, it is classified as a silt of low plasticity.

4.6 Maximum and Minimum void ratios

Tests were conducted according to BS 1377- 4:1990 to obtain the maximum and minimum void ratios of the host sand and the A mixtures. The maximum void ratio

was obtained by pouring dry material in a 1L mould three times and by averaging results.

For determination of the minimum void ratio, a modified proctor test and vibration (method) test were used. For the modified proctor test, a rammer was used to compact the silt sand mixture in a 1L-mould. For the vibration test, the mixture was poured in a 1L mould and compacted with a vibrating hammer for at least 2 min until there was no further significant decrease in sample height. Minimum void ratios obtained by modified proctor testing were found to be higher compared to results obtained by vibrating hammer testing (see figure 4.9). However, the vibrating hammer testing procedure is not suitable for mixed soils with fine content more than 10%, because of fines are likely to escape from the sample during the vibration (BS-1377-4; 1990). Therefore the vibrating hammer procedure was modified so that the amount of fines escaping from the 1L mould was limited. This modification was obtained by reducing the amount of water used during compaction. The mixed soils were compacted under initial water content as described on BS 1377:1975 Test 14 (Head, 1980). This is justified, since the final maximum dry density depends on compaction energy and not on water content (Drnevich, 2007). Further, in this report, the minimum void ratios determined with the modified vibrating hammer are used.

It was found difficult to determine the maximum and minimum void ratios of mixtures B because mixtures B are so cohesive that compaction by vibrating hammer or proctor rammer does not work on them. Therefore, it is assumed that they have the same maximum and minimum void ratios versus fines content curves as the mixtures A which is likely to be not correct: They have the same host sand but their fines present different grain size distribution and mineralogy.

Fig 4.9 presents the minimum and maximum void ratio versus fines content for the quartzic source materials and their mixtures. The maximum void ratio curve shows a trough for fines contents between 15 and 30%. Outside this range, the minimum void ratio increases sharply. In comparison, the maximum void ratio varies less despite decreasing to a minimum at about 30% fines content before increasing slightly at

high fines contents. For these high fines contents, the angular nature of the fragmented silts allows the abstention of loose mixtures. Nevertheless, these mixtures do not bulk when compacted and can achieve a compact packing.

From figure 4.8, the mixtures between 15%-30% fines contents are expected to have lower compressibility because they show the lowest maximum void ratio and are able to reach the lowest void ratio under compaction.

In figure 4.9, the curves of the extreme void ratios versus fines contents are compared to curves obtained for other mixtures by others. The extreme void ratio for clean sands exist in a wide ranges as it can be seen from fig 4-9 and 4-10.The data difference may be due to difference on the size and shape of fines and sand used in mixtures. However, all curves show a more or less pronounced trough. That of the maximum void ratio for the A mixtures manifest the most prominent trough.

The void ratio evolution can be seen from left to right of figure 4-8 and 4-9.From pure sand void ratio on the left to pure silt on the right. From left, the void ratio decreases since part of sand grains voids are filled by fines .At the trough, the fines fills the void that is made available by coarse grains. For large values of fines content, sand grains are replaced by equivalent bulk volume of fine grains.

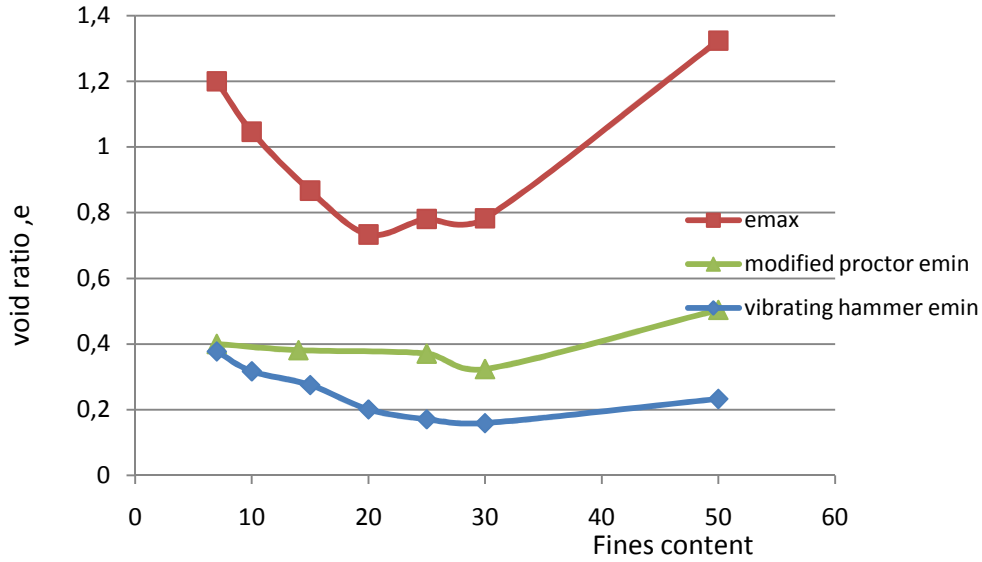

Fig 4. 8 Maximum and minimum void ratio used in this study- add results for 0 and 100 % FC

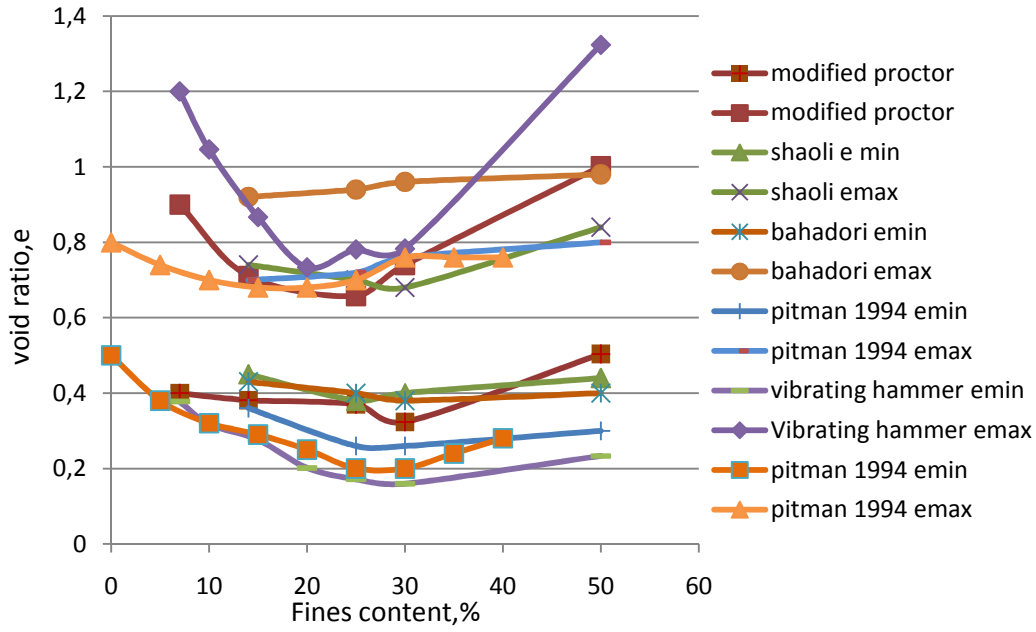

Fig 4. 9 Comparison between the maximum and minimum void ratios observed in this study and published values for other soil mixtures.

4.7 Compression properties of tested material

Table 4.4 shows the compression properties of the host sand, artificial silt and Belgium silt. It can be seen that the compression index of the Belgium silt is higher compared to that of the host sand which is itself higher than that of the artificial silt.

Table 4- 4 Typical compression index of host materials at 140 kPa

Material	Compressibility Index, -	Coefficient of secondary compression, -
Host sand	0,07	0,001
Artificial Silt	0,04	0,003
Belgium silt	0,15	0,019

Chapter 5

Sample preparation and testing

To get undisturbed mixed samples from field for laboratory testing is difficult. An alternative approach is to test reconstituted samples obtained by mixing sand with various quantities of fines.

5.1 Experimental strategy

As mentioned above, the reconstituted samples were created by mixing sand with different portions of silt and clay. Mixing was done to obtain gap graded materials (see section 4.4) which are homogenous and easy to saturate. Gap grading is a characteristic of mixed soils found in hydraulic reclaimed fills (Vos, 2009, pers comm.).

The compressibility tests were performed at different relative densities (30%, 50% and 65%) for the mixtures A and at a relative density assumed to be of 50% for the mixtures B. All samples were created using the slurry deposition method that simulates well hydraulic deposition mode of sediments (see section 4.4).

Oedometer tests were conducted with loading steps ranging from 3.5 KPa to 1.1 MPa. The relevant load for hydraulic fills is about 140 kPa, but tests were also continued up to higher stresses to better capture the behaviour of mixed sands.

5.2 Procedures to create samples

The water content was used as controlling parameter, because water content influences directly the void ratio of the mixture which then influences its relative density. The void ratios corresponding to relative densities of 30%, 50% and 65% were derived from figure 4. 9 and are shown in figure 5.1 for different fines contents.

The void ratio was set according to the equation 1 below

$$e_{target} = e_{\max} - D_r (e_{\max} - e_{\min}) \qquad (5.1)$$

Where e_{target} =Targeted void ratio

D_r = Targeted relative density

e_{max} =Maximum void ratio

e_{min} =Minimum void ratio

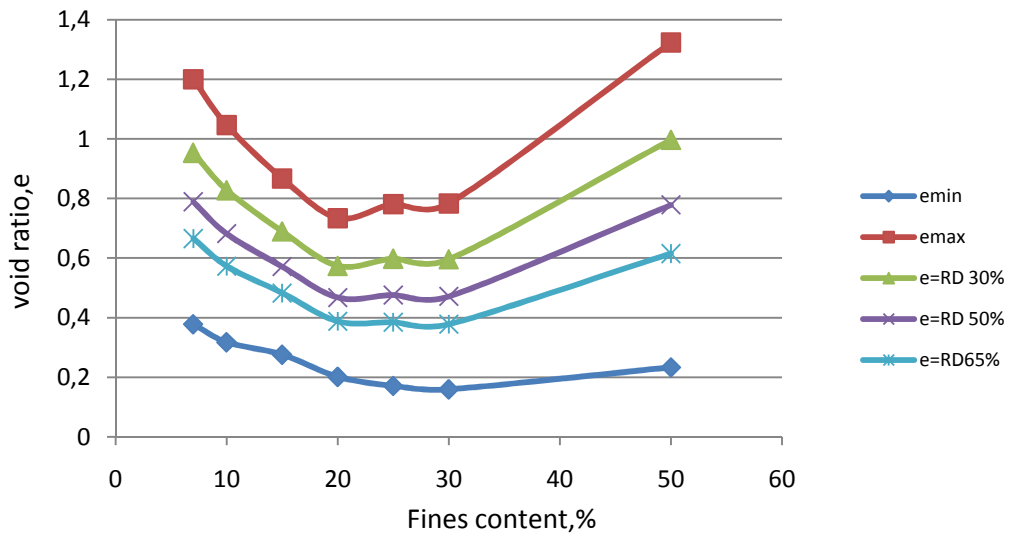

Fig 5. 1 Targeted Void ratios for sample testing

Samples were created following the procedure used by Monkul et al (2007) in batches of 6 kg in weight.

- Dried weights of sand and silt needed for the desired fines content are estimated.

  Fines content (FC) refers to percentage of fine grains in total weight of solids.

$$FC,\% = \frac{FC}{sand + FC} x100 \qquad (5.2)$$

Where, $FC,\%$ =Fines contents in percentage

FC = amount of fines in mixture

$sand$ = Amount of sand in the mixture

- The required quantities of sand and silt are weighted.
- Then, the dry sand and silt are mixed for 10 to 15 minutes, until the mixture is observed to be visually homogenous
- Tap deaired water is added to the mixture. The amount of water added to the dry material defines the water content of the sample and thereafter the void ratio and relative density of the mixture. The mixture is soaked in 24 hrs
- Then, wet mixing is performed for 15 minutes in such a way that sand grains are dispersed in the mixture uniformly and segregation is prevented.
- The slurry is poured into the oedometer mould with a spoon.

However, during sample preparation for oedometer testing a problem was spotted: the oedometer sample created had either high water content or a low water content; this led to the shifting of targeted void ratio and relative density. As a result, the sample taken for testing had either too high or too low fines content depending on water content in the sample. It was found difficult to control water content, fines contents and relative density of samples created by this method. A new preparation procedure was adopted.

The new procedure is identical to that presented above, except that, rather than creating a sample in a bulk of 6kg as Monkul et al (2007) did, a small quantity of mixed soil requiring 100g of dry mixture is prepared for a specific test.:. By this way, the void ratio and fines content of the sample are better controlled.

The specific gravity of all grains is considered constant and equals to 2.67. The oedometer samples are considered to be full saturated; therefore, the only parameter that has to be controlled is the void ratio that is derived from the water content. Figures 5.2-5.4 show photographs of the prepared mixtures.

Fig 5. 2 Mixture A prepared with artificial silt at a relative density

50

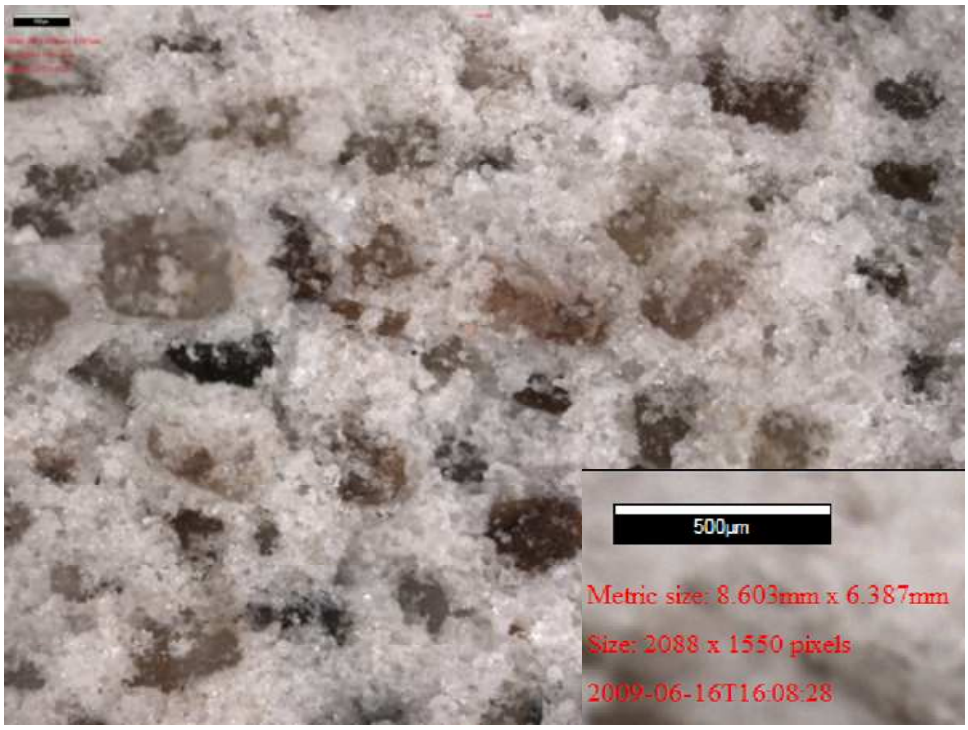

Fig 5. 3 Zoom of mixture A shown in previous figure

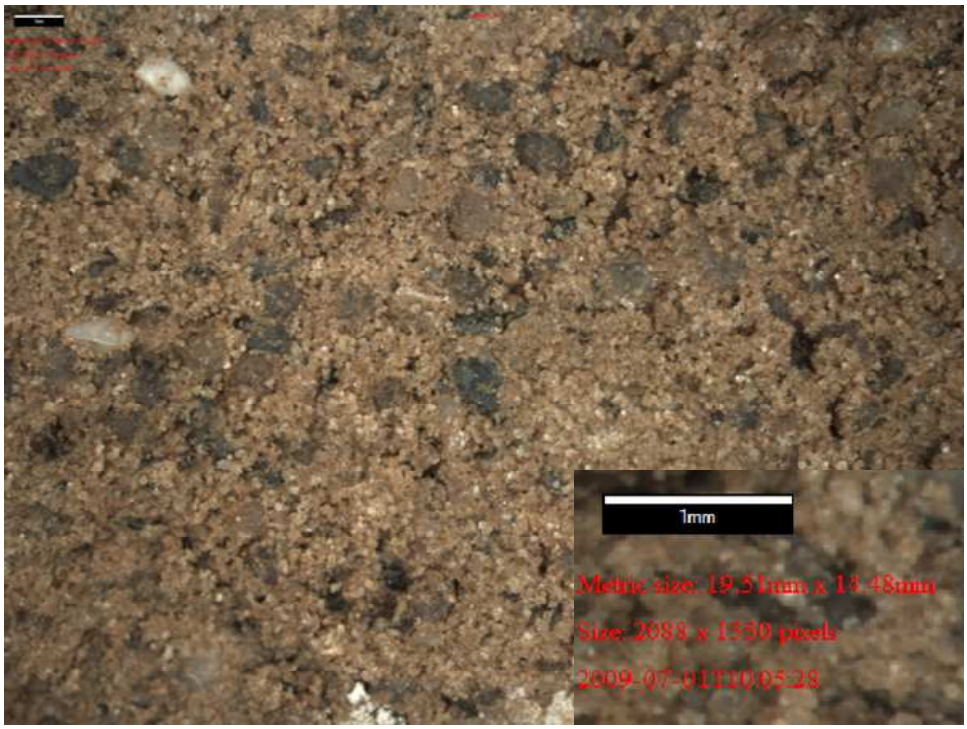

Fig 5. 4 Mixture B prepared with Belgium silt at a relative density 50

5.3 Oedometer Testing

For oedometer testing, the soil specimen is enclosed in a 20 mm high and 63 mm diameter brass ring. The inside of the ring is lubricated with silicone grease to minimize the side friction between the ring and soil specimen. Filter papers are placed on top and bottom of the soil specimen to prevent particles from being forced into the pores of the porous stones placed on both sides of the specimen. The porous stones were once boiled in deaired water and saturated under vacuum. Afterwards, in between two tests, the porous stones are kept in distilled water to maintain their saturation.

The ring containing the sample is prepared as described above. A loading cap is placed onto the ring. The ring is then placed in a consolidation cell and screwed tightly to close the fitting metal jacket on top of the cell. The cell is then mounted and positioned in the loading frame (fig 5.5). The loading yoke is placed on the loading cap and by placing deadweights on the hanger the specimen is loaded axially. Because of the length of the lever arm the applied weight is multiplied by a factor, depending on which hole of the beam the hanger is connected to. A vertical deflection dial gauge is fixed in position to give readings of the vertical settlement under application of loads. The cell is inundated with distilled water and a nominal load of 3.5 KPa is applied. The following vertical stresses are applied: 6.9, 13.9, 34.6, 69.3, 138.5, 277.1,554,2 and 1108.3 kPa. The vertical stress is held constant during approximately 30 minutes, which is generally sufficient to obtain the creep data of the sandy soils tested. During oedometer process, the soil sample is compressed axially and water drains out of the specimen, resulting in a decrease in height which can be measured with the displacement transducer at suitable intervals. These intervals are geared to the Taylor and Casangrande method but should be suitable to determine the stress - strain - creep characteristics.

While testing mixtures A and B, no unloading-reloading loops were followed. The consolidation tests were conducted in a room maintained at a temperature of 17.8 ^{0}C.

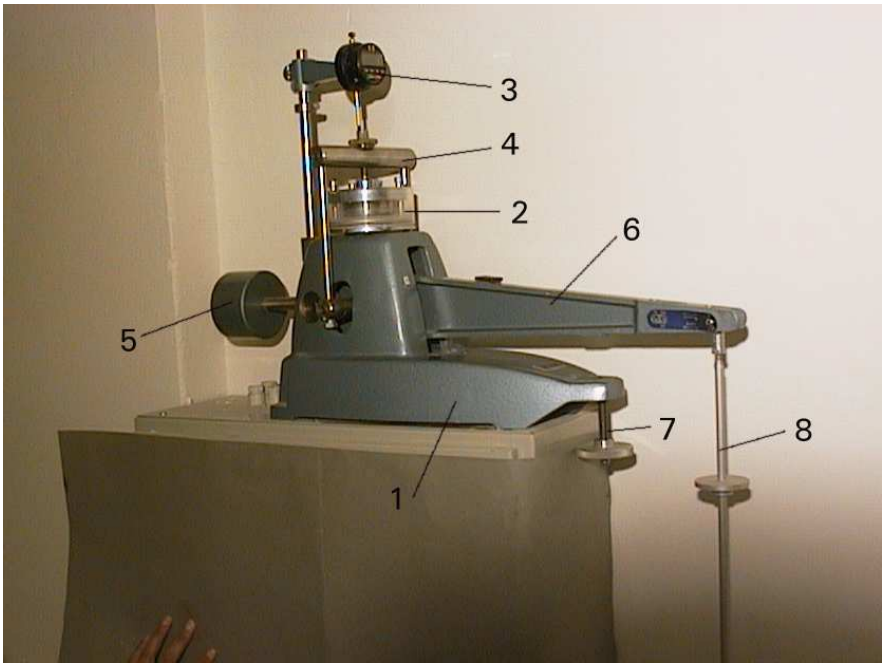

Fig 5. 5 Oedometer test equipment

1- frame of device
2- oedometer cell
3- displacement transducer
4- loading yoke
5- counter balance weight
6- lever arm
7- lever arm support screw
8- deadweight hanger

After the testing, the sample is dried in an oven to measure the sample water content after test. Furthermore, the mass of sample obtained after drying is useful in back analysis of the condition of sample before the testing. This is done by taking in account the initial mass of the sample and the mass after drying. Assuming that no particles were lost, initial water content of the sample during the test is calculated

and compared to the estimated initial water content and if necessary, the initial void ratio is corrected.

Tables 5-1 to 5-4 give an overview of the sample conditions of the A and B series of oedometer tests. The values of the targeted initial void ratios can be compared to obtained values.

Table 5- 1 Mixture A samples for oedometer testing at relative density-30%.

sample	silt	Minimum void ratio	Maximum void ratio	Initial water content	Initial density	Initial dry density	Initial void ratio	Relative density
	%	-	-	-	kg/m3	kg/m3	-	%
A24	7	0,378	1,4	0,41	1791,7	1270,7	1,09	30
A25	10	0,318	1,046	0,31	1906,5	1455,4	0,83	30
A19	15	0,276	0,867	0,20	1924,8	1604,0	0,658	35
A26	15	0,276	0,867	0,25	1968,1	1574,5	0,69	30
A20	20	0,201	0,734	0,20	2061,4	1717,9	0,548	35
A27	20	0,201	0,734	0,21	2046,2	1691,0	0,57	30
A21	25	0,171	0,781	0,15	1929,4	1672,7	0,590	31
A28	25	0,171	0,781	0,23	2014,1	1664,5	0,60	30
A22	30	0,160	0,783	0,21	2001,3	1654,0	0,608	28
A29	30	0,16	0,783	0,22	2040,0	1666,7	0,60	30
A23	50	0,233	1,323	0,14	1339,8	1175,2	1,263	6
A30	50	0,233	1,323	0,37	1825,4	1332,4	1,00	30

Table 5- 2. Mixture A samples for oedometer test at relative density of 50%.

sample	silt	Minimum void ratio	Maximum void ratio	water content	Initial density	Dry density	Initial void ratio	Relative density
	%	-	-	-	kg/m3	kg/m3	-	%
A10	10	0,318	1,046	0,20	1932,9	1610,8	0,651	54
A11	10	0,318	1,046	0,20	1752,2	1642,7	0,619	59
A12	15	0,276	0,867	0,21	2065,6	1700,4	0,564	51
A13	20	0,201	0,734	0,18	2175,0	1843,2	0,443	55
A31	20	0,201	0,734	0,17	2120,7	1812,6	0,468	50
A14	25	0,171	0,781	0,20	2147,8	1789,8	0,486	48
A32	25	0,171	0,781	0,18	2126,4	1802,1	0,476	50
A15	30	0,16	0,783	0,17	2143,5	1786,2	0,489	47
A16	30	0,16	0,783	0,17	2143,5	1786,2	0,489	47
A33	30	0,16	0,783	0,18	2115,2	1792,6	0,484	50
A17	50	0,233	1,323	0,20	1901,5	1584,6	0,679	59
A18	50	0,233	1,323	0,20	1901,5	1584,6	0,679	59
A34	50	0,233	1,323	0,29	1929,6	1495,8	0,778	50

Table 5- 3 Mixture A samples for oedometer test at relative density of 65%

sample	silt	Minimum void ratio	Maximum void ratio	water content	Initial density	Dry density	Initial void ratio	Relative density
-	%	-	-	-	kg/m3	kg/m3	-	%
A1	7	0,378	1,4	0,16	1944,2	1676,0	0,515	85
A2	7	0,378	1,4	0,19	1878,9	1765,9	0,506	86
A3	7	0,378	1,4	0,27	2021,0	1591,4	0,672	68
A4	10	0,318	1,046	0,22	2053,1	1682,9	0,581	63
A5	15	0,276	0,867	0,19	2069,1	1739	0,530	57
A6	20	0,201	0,734	0,15	2159,5	1884,8	0,411	61
A7	25	0,171	0,781	0,14	2101,2	1835,8	0,449	54
A8	30	0,16	0,783	0,14	2141,4	1871,5	0,421	58
A9	50	0,233	1,323	0,23	2076,9	1688,5	0,575	69

Table 5- 4 5 Mixture B samples for oedometer testing at 50% relative density

sample	silt	Minimum void ratio	Maximum void ratio	water content	Initial density	Dry density	Initial void ratio	Relative density
	%	-	-	-	kg/m3	kg/m3	-	%
B1	7	0,318	1,046	0,20	1932,9	1610,8	0,651	54
B2	10	0,318	1,046	0,20	1752,2	1642,7	0,619	59
B3	15	0,276	0,867	0,21	2065,6	1700,4	0,564	51
B4	20	0,201	0,734	0,17	2120,7	1812,6	0,468	50
B5	25	0,171	0,781	0,18	2126,4	1802,1	0,476	50
B6	30	0,16	0,783	0,18	2115,2	1792,6	0,484	50
B7	50	0,233	1,323	0,29	1929,6	1495,8	0,778	50

5.4 Problems encountered

Segregation and air bubbles

The following observations were made for the different targeted relative densities;

- At a relative density of 30%, samples showed segregation of sand and fines, they presented alternating layers of coarse and fine materials.
- At a relative density of 50%, samples were uniform; they showed no segregation, and no air entrapment. See figure 5.2
- At a relative density 65%, samples were uniform and homogenous, but they suffer from air entrapment and contained large voids due their low water content.

The segregation problem could not be solved and it was decided to put tless emphasis on the test results obtained at a relative density of 30%. The air entrapment problem was considered not to have a huge influence on the sample compressibility.

Targeted void ratio

Initially, it was proposed to create samples based on Monkul et al (2007)'s work. A 6 kg sample was created and soaked for one day and afterward the specimens were taken from the bulk sample to the oedometer cell. When studying material behavior, it is important to have a controlling parameter, in this case the void ratio or relative density. The controlling parameter can be done by controlling the specimen water content; the desired void ratio can be obtained.

However, while placing the sample in the odometer cell, it was observed that the sample had a different void ratio which deviated from the targeted void ratio. Either the sample had a higher or lower void ratio than expected. Back analysis of the sample initial testing conditions after finishing testing was performed to calculate the initial condition of the sample tested. Back analysis was based on the water content of the remaining part of the sample and water content of a sample after testing and void ratio measured based on oedometer ring. All these data were compared and the difference was analyzed and given out.

This led to the use of the new method of sample preparation, in which water content and therefore void ratio were controlled properly.

Fines escape from the sample in oedometer cell

After placing the sample in the oedometer cell, fines were escaping from the sample. This affected mostly the samples of low fines contents where fines were segregated and escaped with water during placement of the oedometer cap.

Solution for this was to perform a test in high relative density were water content in the sample is low. Tests performed with a low fines content at a high relative density and therefore with a low water content in the sample led to more reliable results

Sand particle between the oedometer ring and cap

The presence of sand particles in between the cap and the wall of the oedometer ring causes the system to jam. No vertical displacement was observed. The problem was solved by cleaning the cap and applying lubricant on the cap.

Friction on the sample and the oedometer ring

Friction between the sample and the oedometer ring was observed; Samples having the same physical properties had a different final void ratio. Problem was solved by applying lubricant in the walls of oedometer ring. Application of the lubricant reduces friction but not completely.

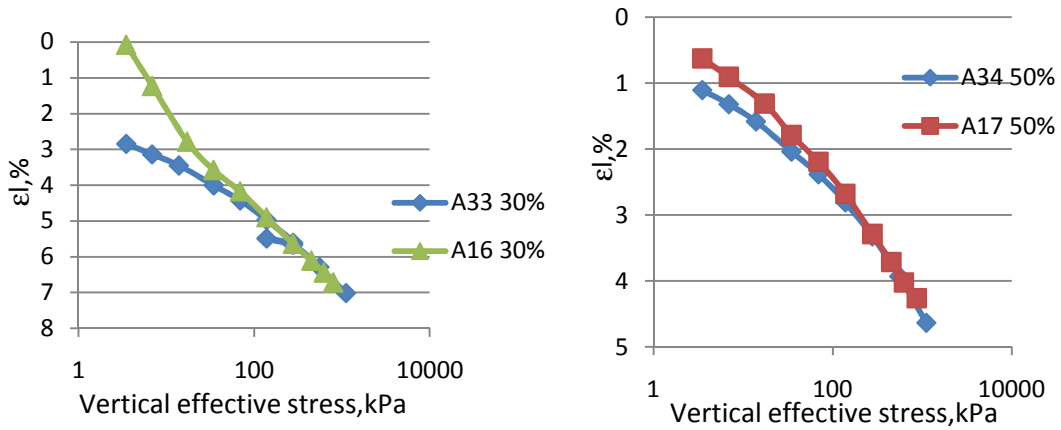

Fig 5. 6 results reproducibility for 30 and 50% fines contents at relative density of 50%

Squeezing of the sample during testing

Sample tends to be in a inhomogeneous way during the testing, especially at low stresses. If the oedometer cap becomes tilted, oedometer compression is not homogeneous in the entire sample. The solution was monitoring the tests during the first loading steps and reassembling the sample, the ring and the cap if necessary.

Height of sample in a conventional incremental oedometer test

It was observed to be difficult to measure exactly the height of the sample in the oedometer cell. This brings to the difficult in estimation initial condition at which sample was tested. Most of samples show some void ratio shifting because of an accuracy of measuring the height of the sample in the oedometer cell.

Chapter 6

Analysis of laboratory test results

The hypothesis made for this research states that "**fines mixed with sand to a certain ratio that is greater than 1 to 10 increases the compressibility and secondary compression of the sandy mixture"**. In this chapter, oedometer data gathered to support this hypothesis is presented and analyzed. First, general trends that were observed are exposed. Then, the way in which data is analyzed to derive oedometer parameters is explained. Derived parameters are presented. Their variations as function of vertical stress, relative density and fines contents are described.

6.1 Observed results

6.1.1 Relationship between effective stress and vertical strains

The relationship between effective stress and vertical strains for the different materials tested at different relative densities and fines contents is shown in figure 6.1. The mixtures A were tested at different relative densities but the slope of their virgin compression curves don't show any trend as function of fines content. The B mixtures were tested at an assumed relative density of 50%,; the compression line steepness increases with an increase in fines content.

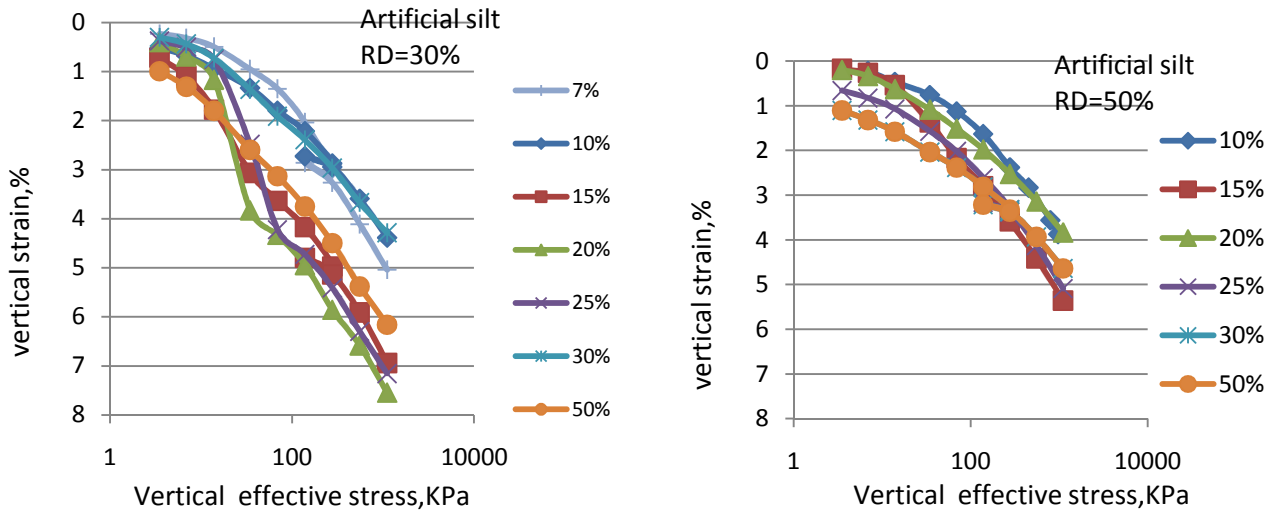

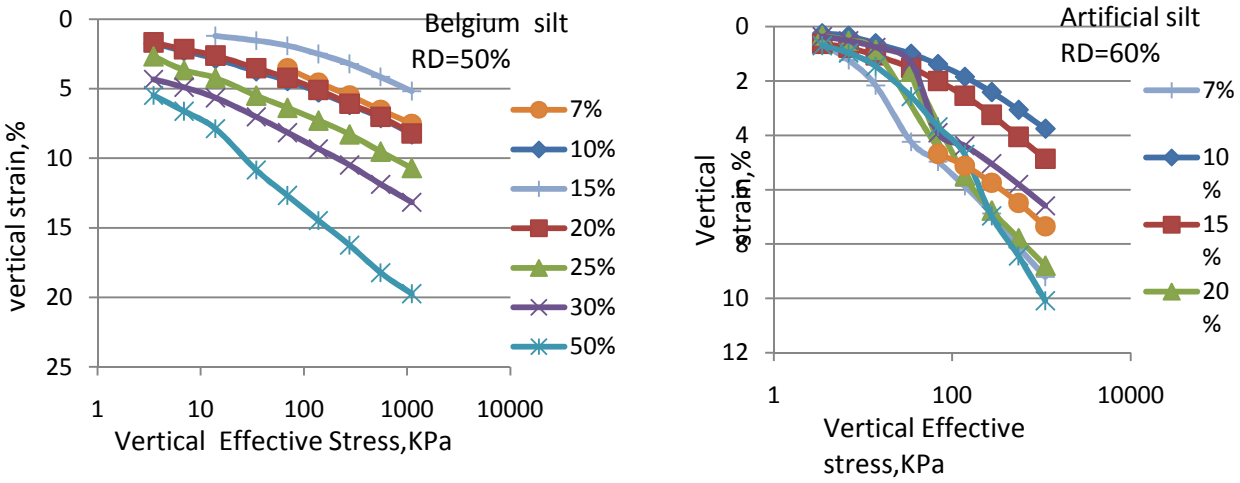

Fig 6. 1 . Relationship between vertical strain and vertical effective stress recorded during oedometer testing on the A and B mixtures.

From figure 6.1, it can observed that the mixtures A tested at a relative density of 50% are less compressible compared to the mixtures B (assumed to be) tested at the same relative density.. The reason for this difference in compressibility can be attributed to difference in mineralogy, grain distribution and/or grain size and shape.

During tests conducted at low relative density (30%), fines tend to escape from the sample and grain segregation occurs. The test results are less reliable.

6.1.2 Relationship between void ratio and vertical effective stress

Figure 6.2 shows the relationship between void ratio and vertical effective stress. The initial void ratios are as expected, considering the targeted void ratios.

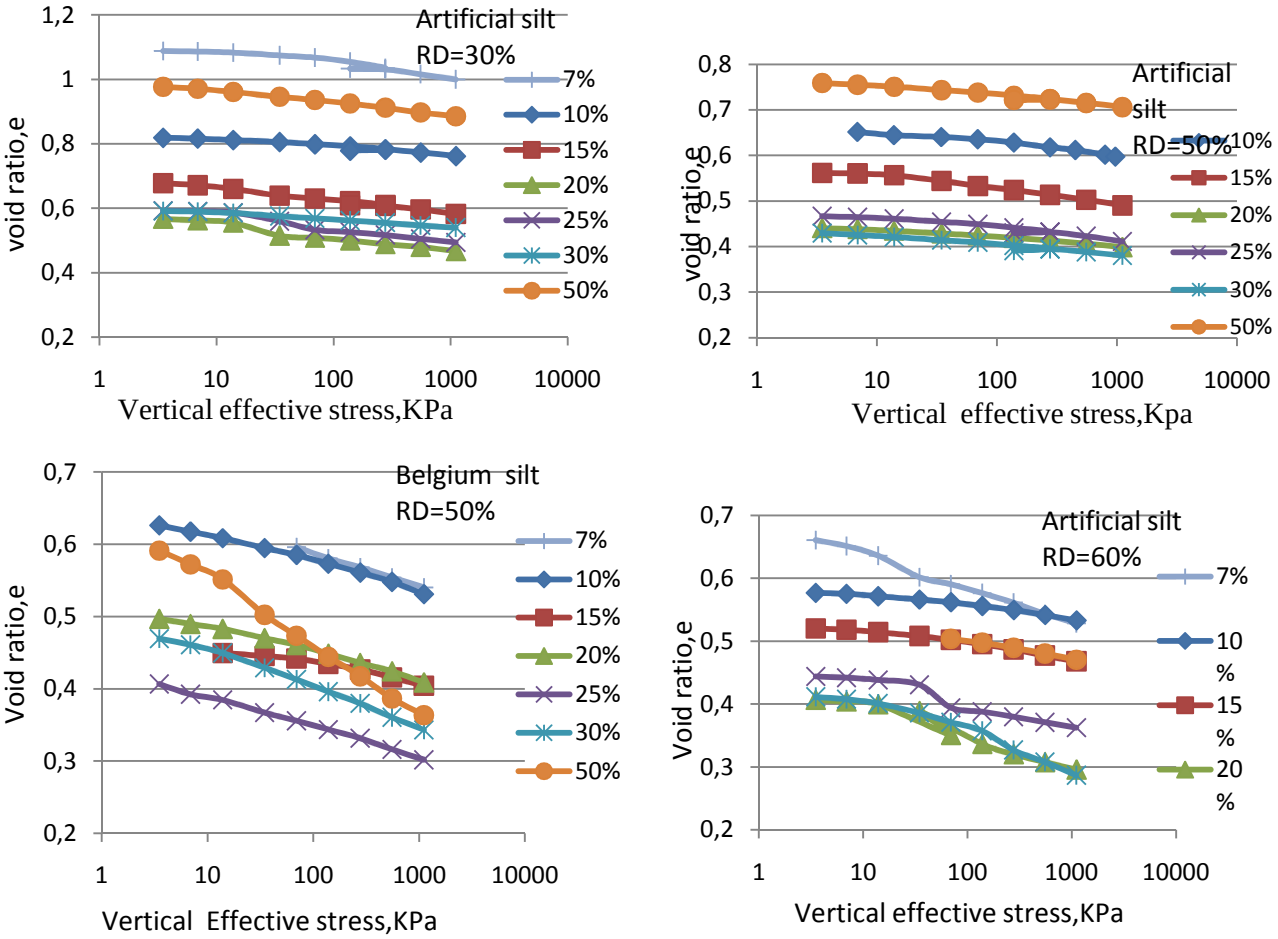

Fig 6. 2 Relationship between void ratio and vertical effective stress recorded during oedometer testing on the A and B mixtures.

6.2 Parameters determination

6.2.1 Primary compression

Primary compression is expressed in terms of, the coefficient of consolidation, C_v, the coefficient of volume compressibility, m_v or its inverse, the oedometer stiffness, E_{oed} and the compression and recompression indices, C_c and C_r, respectively. Primary compression occurs during the increase in effective stress.

Coefficient of consolidation, *Cv*

The coefficient of consolidation C_v is a measure of time it takes for a soil to consolidate during the lab test. The coefficient of consolidation is determined based on Taylor time method (BS 1377; 1990; 4). This method is based on the time for 90% consolidation used because 90% consolidation represents a large portion of primary consolidation stage and in oedometer testing, 90% consolidation is achieved in relatively short time as shown in the fig 6.3.

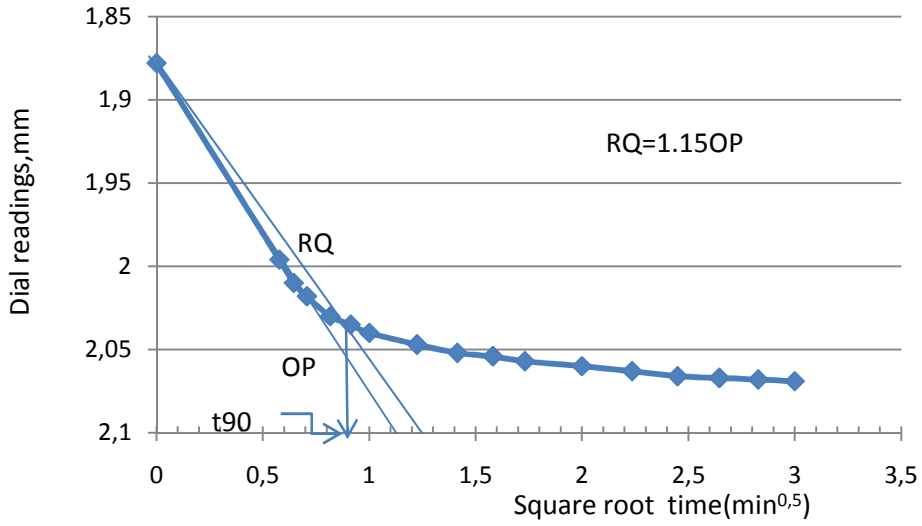

Fig 6. 3 determination of Coefficient of consolidation, C_v by Taylor time method

The coefficient of consolidation is calculated using equation (6.1):

$$Cv = \frac{0.111 H^2_{av}}{t_{90}}, \quad m^2 / year \tag{6.1}$$

Where H_{av} is the average height in mm of the sample in particular loading step,

t_{90} is the time determined from Taylor time method from fig 6.3 and expressed in min.

Coefficient of volume compressibility, m_v

The coefficient of volume compressibility m_v is defined as the volume change per unit volume per unit increase in effective stress. If, for an increase in effective stress from σ'_o to σ'_1 the void ratio decreases from e_0 to e_1, then the coefficient of volume compressibility is expressed as follows:

$$m_v = \frac{1}{1+e_o}\left(\frac{e_o - e_1}{\sigma'_1 - \sigma'_o}\right), \quad m^2/MN \tag{6.3}$$

Its inverse is the oedometer stiffness.

Recompression index (Cr) and Compression index (C_c)

The compression index and initial recompression indices are determined by Casangrande method as sketched in fig 6.4. Fig 6.4 represents the void ratio as function of vertical effective stress. C_r and C_c are the slopes of the linear portion of the curve before and after preconsolidation stress (σ_p), respectively.

The compression index is calculated using equation (6.2):

$$C_c = \frac{e_o - e_1}{\log \frac{\sigma'_1}{\sigma'_o}}, \quad - \tag{6.2}$$

The recompression index can also be calculated as the slope of the reloading curve of an unloading-reloading cycle.

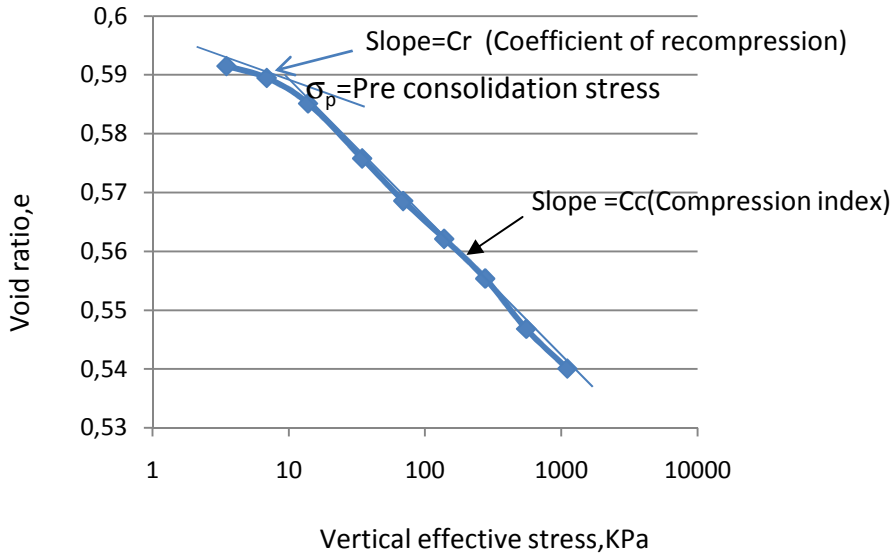

Fig 6. 4 Determination of compression and recompression indices.

6.2.2 Secondary compression

In secondary compression, the soil structure is subjected to a viscous or creep deformation under action of sustained stress as fabric elements adjust slowly to a more stable arrangement. The rate of secondary compression is controlled by the rate at which the structure is deformed as opposed to the rate of primary consolidation controlled by Darcy's law, which determines how rapidly water can escape from the pores under a hydraulic gradient. The mechanism of secondary compression involves sliding at interparticles contacts, expulsion of water from micro fabric elements and rearrangement of adsorbed water molecules and cations into different positions (Mitchell, 1993).

Coefficient of secondary compression

The coefficient of secondary compression is determined by the slope of the line of the $(e - \log t)$ curve for time greater than t_{90} as sketched in fig 6.5.

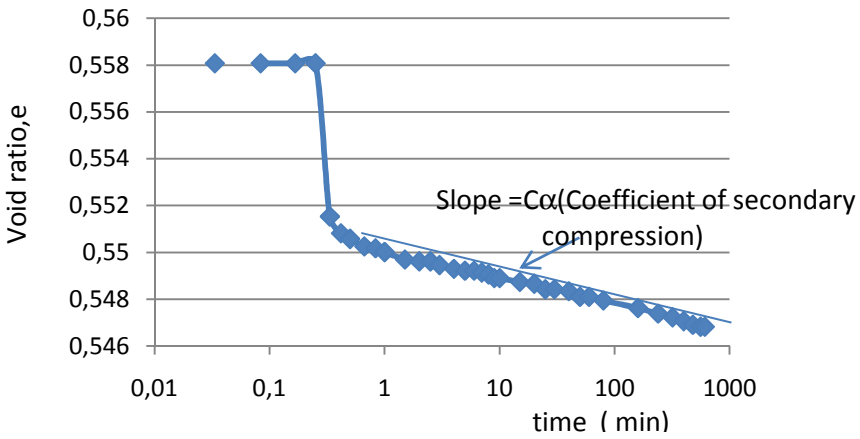

Fig 6. 5 Determination of secondary compression

Chapter 7

Data analysis and Interpretation - Primary compression.

In this chapter the data analysis and interpretation for primary compression is done. The analysis of observed data is done by analyzing the data for vertical effective stresses of 140 kPa and 1108 kPa. The choice of the vertical effective stress of 140 kPa is done to simulate the stresses observed in hydraulic reclaimed fills and the vertical effective stress of 1108 kPa is done to observe the effect of fines on soil behavior at higher stresses. In data interpretation, the results obtained from other researcher are compared with results obtained from this research.

7.1 Oedometer stiffness

Figure 7. 1 shows the relationship between oedometer stiffness and vertical effective stress for the mixtures A and B. As expected the oedometer stiffness increases with an increase in vertical effective stress.

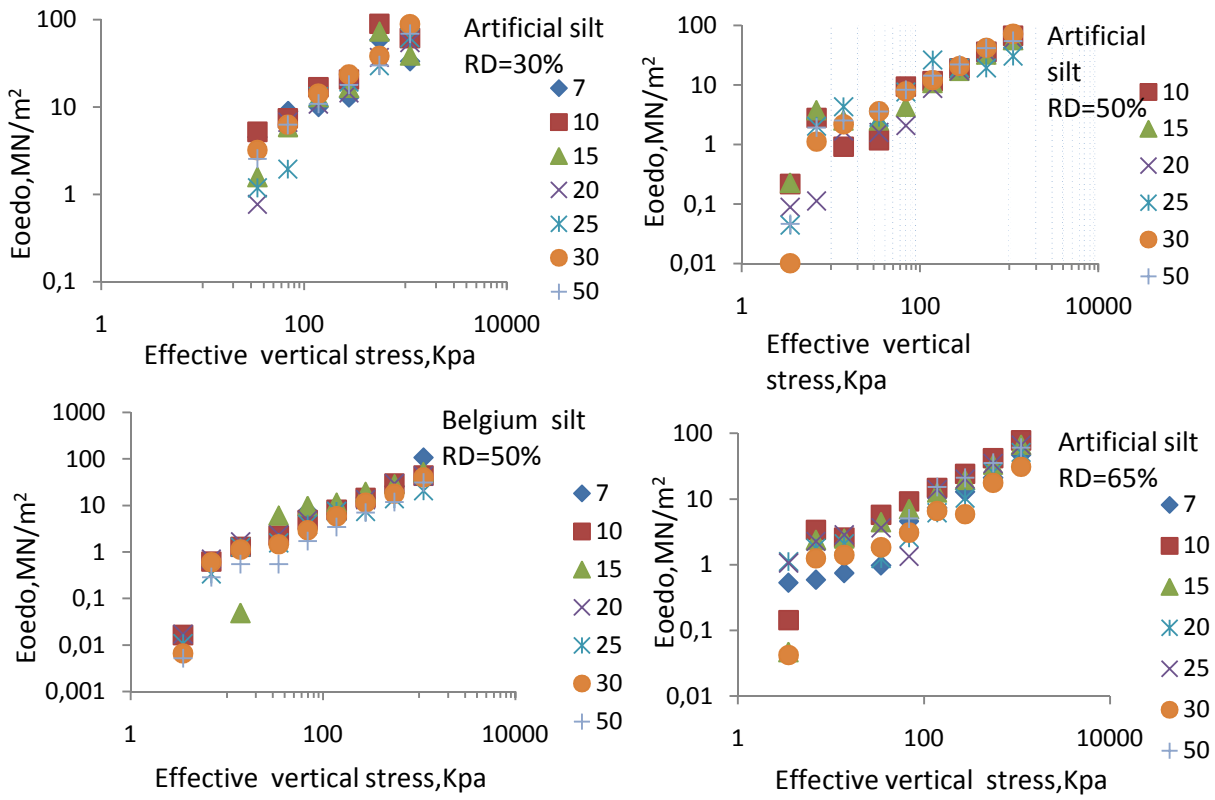

Figure 7. 1 Relationship between oedometer stiffness and vertical effective stress.

In Table 7. 1, the values of oedometer stiffness for the A and B mixtures for all the applied loads of 138 kPa and 1108 kPa are listed. They range from 3.4 -106 MN/m^2.

Table 7. 1 Oedometer stiffness values for different fines contents

	mixtures A						mixtures B	
FC,%	RD=30 %		RD=50 %		RD=65%		RD=50%	
	140kPa	1108,3 kPa	140kPa	1108 kPa	140kPa	1108 kPa	140kPa	1108 kPa
	Eoedo,MN/m^2		Eoedo,MN/m^2		Eoedo,MN/m^2		Eoedo,MN/m^2	
7	9,99	33,51	-	-	7,32	46,62	6,47	106,32
10	16,82	61,55	11,61	67,04	14,72	77,88	8,03	43,84
15	12,97	38,92	10,77	56,42	12,55	66,59	11,58	52,69
20	10,77	54,33	8,71	59,16	6,17	51,19	7,60	42,94
25	13,20	61,81	12,12	30,65	13,88	66,50	7,42	20,63
30	14,18	88,93	20,78	72,12	6,55	30,96	5,84	40,28
50	10,92	68,97	14,44	54,99	15,25	60,62	3,43	31,09

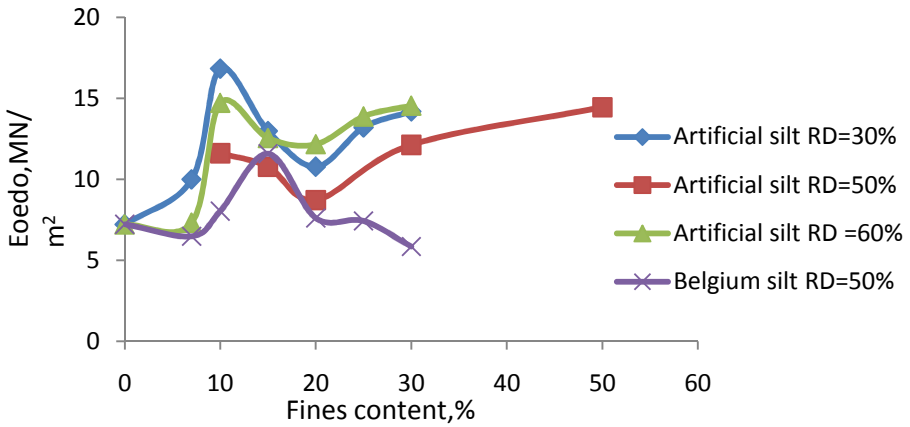

Figure 7. 2 Relationship between oedometer stiffness and fines contents at 140kPa

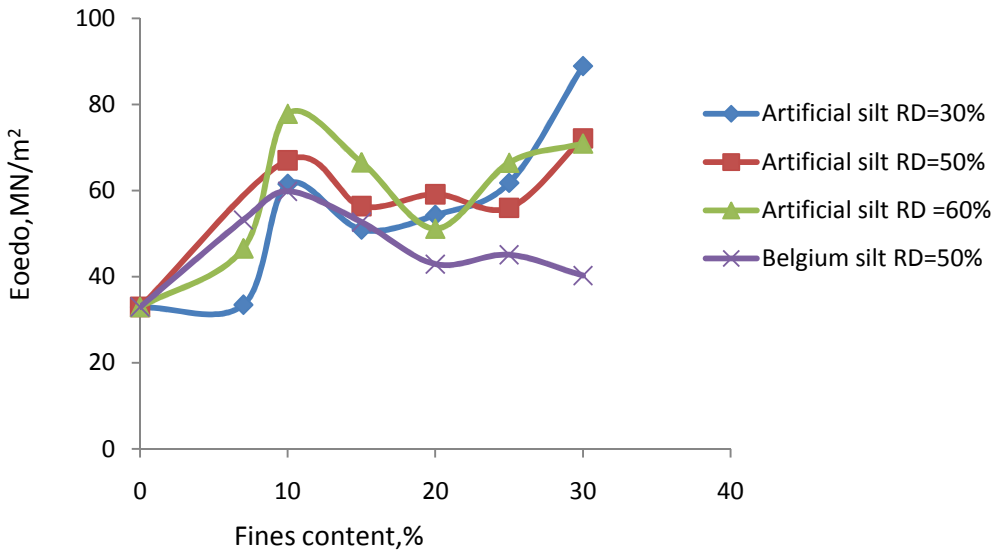

Figure 7. 3 Relationship between oedometer stiffness and fines contents at 1108 kPa

Figure 7. 2 and Figure 7. 3 represent the relationship between oedometer stiffness and fines contents for vertical effective stress of 140 kPa and 1108.3 kPa. Mixtures A present a 'trough' with lower stiffness for a fines content between 10 and 30%. The oedometer stiffness increases between 7 and 10% fines content. Above 30% fines content, the oedometer stiffness increases slightly for 140 kPa and decrease slightly for 1108 kPa. The decrease in oedometer stiffness for fines content between 10% and 30% is due to fact that mixtures at low stress has high compressibility which is caused by fines migration within voids in the mixtures. Mixtures B samples, the oedometer stiffness increases between 7% and 15% and then continually decreases as the fines contents increases for both 140 and 1108 kPa consolidation pressures.

Stiffness decreases initially due to the weak structure formed during fines migration within the mixture voids. The mixture is unstable until voids have been filled by fines and sand grain-grain contact has been established.

The effect of the material type can be observed by comparing oedometer stiffness of the A and B mixtures at 50 % relative density. The mixtures A are found to have a higher oedometer stiffness compared to mixtures B.

7.2 Coefficient of consolidation (C_v)

Figure 7. 4 show the relationship between coefficient of consolidation and vertical effective stress. The coefficient of consolidation decreases with an increase in vertical effective stress for the mixtures A. For the mixtures B , with silt content of 7% to 15% the coefficient of consolidation also decreases with an increase of effective stress while for silt content of 20-50%, it increases with increasing effective stress. This means that the mixtures A and the mixtures B with fines content less than 20% tend to consolidate faster at low stresses and slower at high stresses while the Belgium silt samples with fines contents above 20% tend to consolidates slower at lower stress.

As discussed in previous chapter on presence of mica on Belgium silt samples influences the consolidation behaviour of these mixtures. Mica in Belgium silt samples which are platy can exist in voids between the coarse particles and can be passive and nonload bearing. Under high hydraulic gradient, these passive particles may migrate to create non uniform fabric. Migration of fine particles within the soil matrix may block or unblock interconnected voids and affect results of consolidation (Mitchell, 1993).

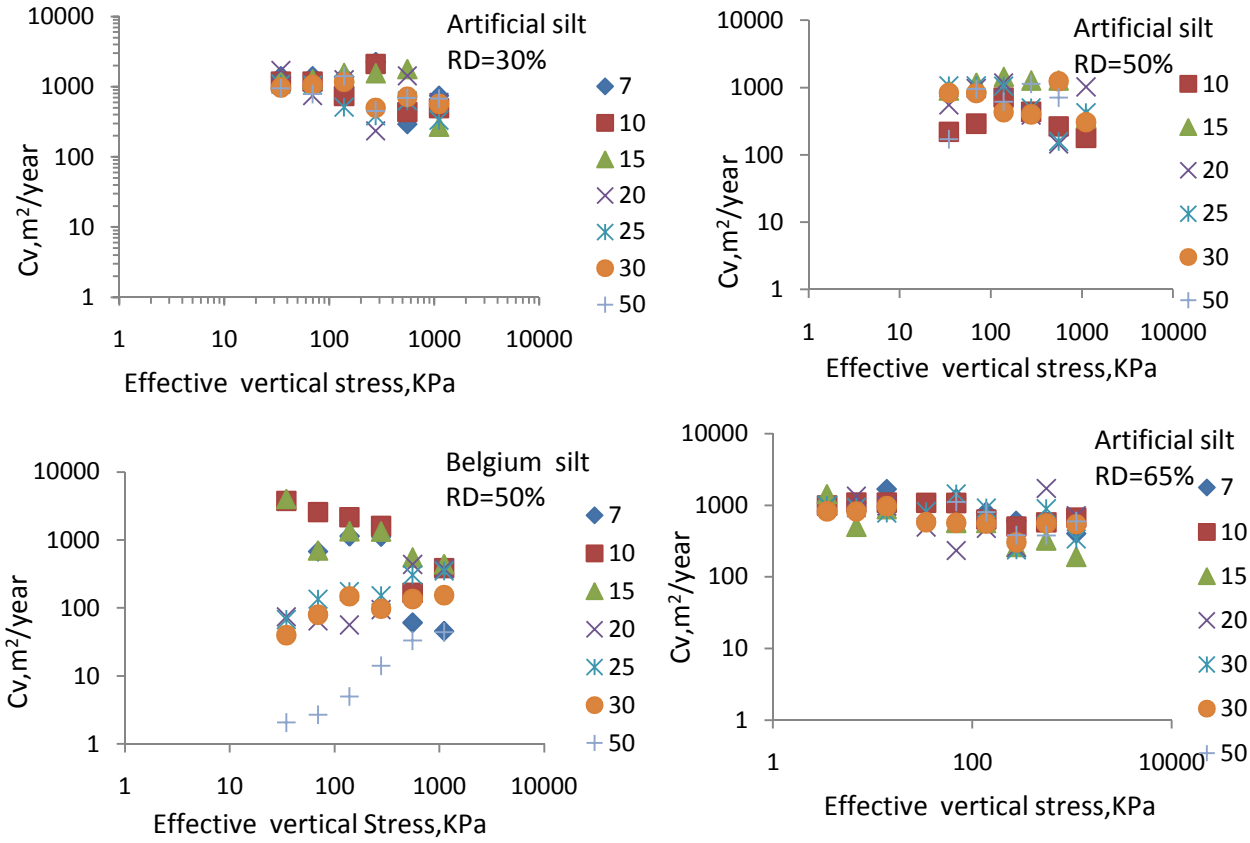

Figure 7. 4 Relationship between C_v and vertical effective stress for the A and B mixture

The coefficient of consolidation values for 140 kPa and 1108 kPa loading steps are listed in table 7.2 **Error! Not a valid bookmark self-reference.**.These values are the same as those listed in table 3.2. They vary between 5 -1441 m^2 / *year* . The lower values are typical of silts soils (Taylor 1948; Head 1982) while the larger values are typical of sandy materials (e.g. Nelson et al 1977; Keshian and Rager 1988).

Table 7. 2 C_v for different soil type, relative density and fines content

	Artificial silt						Belgium silt	
	RD=30%		RD=50%		RD=65%		RD=50%	
FC,%	C_v, m^2/yr		C_v , m^2/yr		C_v, m^2/yr		C_v , m^2/yr	
	140 kPa	1108 kPa	140 kPa	1108 kPa	140 kPa	1108 kPa	140 kPa	1108 kPa
7	1389	743	-	-	806	403	1137	46
10	736	495	710	266	633	673	2161	386
15	1572	271	1438	1268	564	191	1341	440
20	1258	598	1178	1441	475	716	56	376
25	512	334	1049	1300	913	339	174	350
30	1168	571	431	1242	556	541	149	154
50	1408	678	615	711	806	598	5	44

The influence of fines on the coefficient of consolidation can be observed in Figure 7. 5 Figure 7. 6. For the mixtures A, the coefficient of consolidation increases with fines content from 7% to 15%; at a fines content of 15%, it reaches a peak value, then decreases as fines contents increases. For the B mixtures, the coefficient of consolidation reaches a peak value at 10% and then begins to decrease significantly as fines content increases. For the mixtures A, relative density seems to have no influence on the consolidation coefficient.

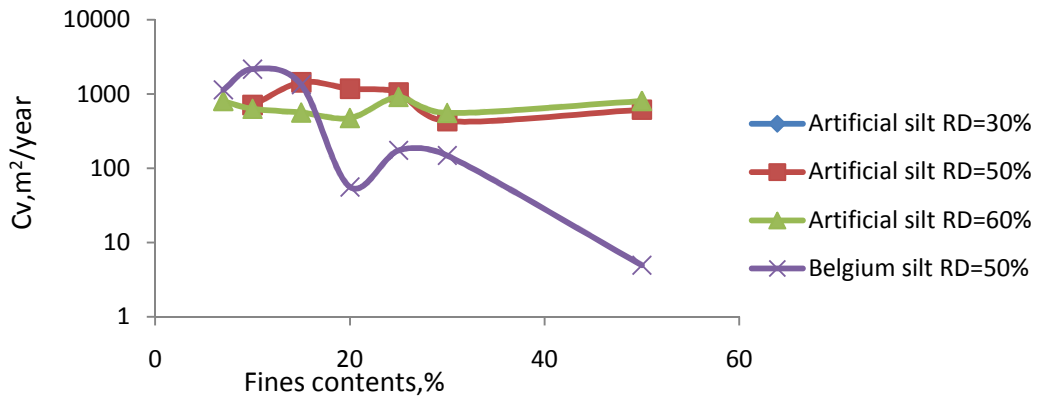

Figure 7. 5 Relationship between Coefficient of consolidation and fines contents for

the mixtures A and B at vertical effective stress of 140 kPa

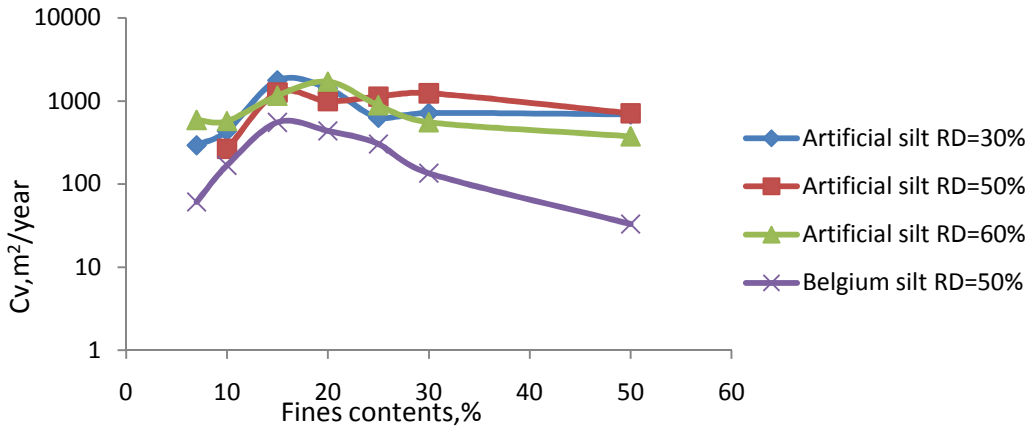

Figure 7. 6 Relationship between Coefficient of consolidation and fines contents for the mixtures A and B at vertical effective stress of 1108 kPa

7.3 Recompression index (C_r)

Table 7. 3 shows the observed C_r values determined at vertical effective stress of 34.6 and 69.3 kPa .The values vary from 0.0044 to 0.0642.

Table 7. 3 C_r-values for different fines content and relative density

	Artificial silt			Belgium silt
Fines content,%	RD=30% C_r,(-)	RD=50% C_r,(-)	RD=65% C_r,(-)	RD=50% C_r,(-)
7	0,0057	-	0,0064	0,0516
10	0,0087	0,0062	0,0048	0,0295
15	0,0212	0,0044	0,0069	0,0100
20	0,0151	0,0061	0,0087	0,0241
25	0,0069	0,0079	0,0071	0,0257
30	0,0068	0,0059	0,0126	0,0290
50	0,0314	0,0126	0,0201	0,0642

Figure 7. 7 show the relationship between C_r, fines contents and the relative density. The values of C_r increases with increasing fines content for all mixtures A except for samples prepared at low relative density. For the B mixtures, C_r decreases with increase of fines content up to 15% and then the C_r increases with an increase of fines content.

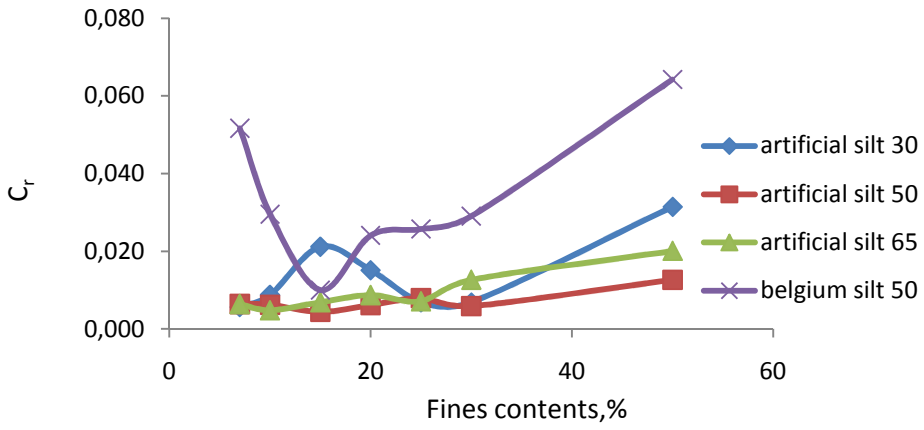

Figure 7. 7 Relationship between recompression index and fines content

Table 7. 4 shows the C_r/C_c values for vertical effective stresses of 34.6 and 69.3 kPa. The C_r/C_c ratio varies according to the relative density at which the material was tested. Its values vary from 0.1-1.11, which is different from the values of 0.02-0.2 reported in literature (Terzaghi et al, 1996) . For clays, high values correspond to the presence of fissure or the process that leads to destructuration and opening of fissure before the control of vertical effective stress is established in the oedometer test (Terzaghi et al 1996). For sands, destructuration is also expected when low stresses are applied. Mixtures B exhibit a high C_r/C_c ratio in comparison to mixtures A. For mixtures A, the highest Cr/Cc values are obtained for 50% fines content whatever the relative density is.

Table 7. 4 C_r/C_c values for different fines content and relative density.

	Artificial silt			Belgium silt
Fines content,%	RD=30% C_r/C_c,(-)	RD=50% C_r/C_c,(-)	RD=65% C_r/C_c,(-)	RD=50% C_r/C_c,(-)
7	0,1066	-	0,1770	1,1133
10	0,2985	0,1986	0,1994	0,6540
15	0,5703	0,1232	0,2486	0,3208
20	0,4408	0,2019	0,1821	0,5574
25	0,2115	0,2593	0,3430	0,5731
30	0,2884	0,2503	0,2779	0,5012
50	0,7500	0,4900	0,8527	0,7034

7.4 Compression Index (C_c)

In this section, the relationship between compression index with effective stress and fines content is discussed. As it known that the compression index increases with increasing effective stress.

Artificial silt RD=30%	Artificial silt RD=50%	Artificial silt RD=65%	Belgium silt RD=50%	Monkul al (2007)
□	-	⤫	◇	▬

Figure **7. 9** show the relationship between the compression index and vertical effective stress for different fines content and relative density. For most tests, C_c first increases rapidly, and then decreases slightly before remaining fairly constant as effective stress increases.

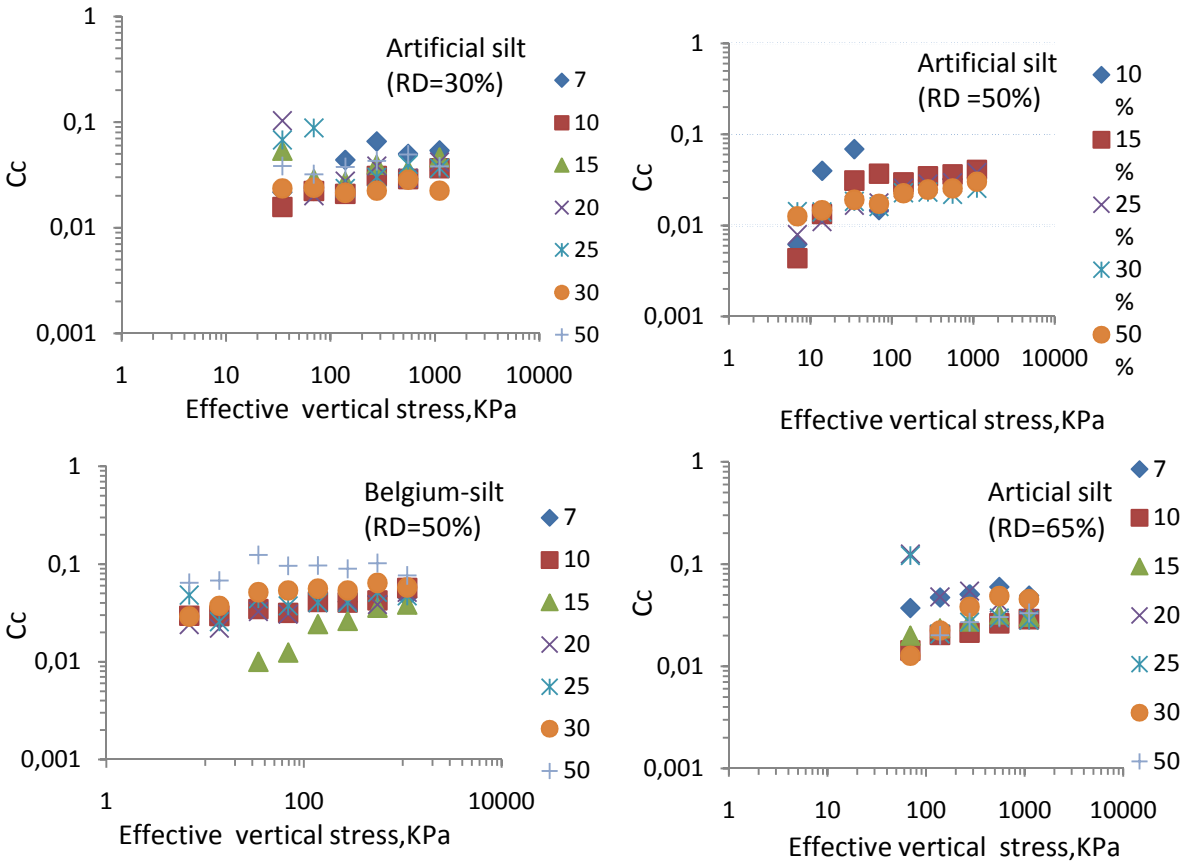

Figure 7. 8 Relationship between compressibility index and Vertical effective stress.

From figure 7.9 ,the values of compression index as function of effective vertical stress are plotted ,the mixture of silt sand used in this research is compared to the two groups of sand published by Mesri and Vardhanabhuti (2009) namely quartz sand and quartz sand with fines content with 10 to 20% ,samples were divided into different groups of loose and dense samples. The shapes of sand grains tested were rounded to subrounded and angular to subangular. This plot was made for compression index of lower stresses between 0.003-1.5 MPa which is equivalent to stress obtained in reclamation fills and it is divided into relative densities of 0%, 50% and 100%.As one can see, loose samples falls in zone of relative density of 0 to 50% where as dense samples falls in the zone of relative density of 50 to 100%.Likewise the sample which are well rounded to subrounded falls in the zone where it corresponds depending whether it is loose or dense.

As one can see ,the mixtures of artificial silt sample doesn’t fall in a zone of quartz with fines content as expected instead the mixtures fall in compression index of quartz sand. The compression index data for the soils tested by Monkul et al (2007) (quartz sand with kaolin as fines) falls within the quartz sands with fines zone. The influence of relative density is not observed as one can see that all sample fall in one band except for Belgium silt sample which are falling in zone of quartz sand with fines content.

Therefore, from the figure 7.8, it can be concluded that fines mineralogy has influence on the compressibility as it can be seen that sand silt mixture with plastic fines have higher value of compression index and is falling in quartz sand with fines zone while samples with non plastic fines the compression index is low and will fall in a zone of loose sand.

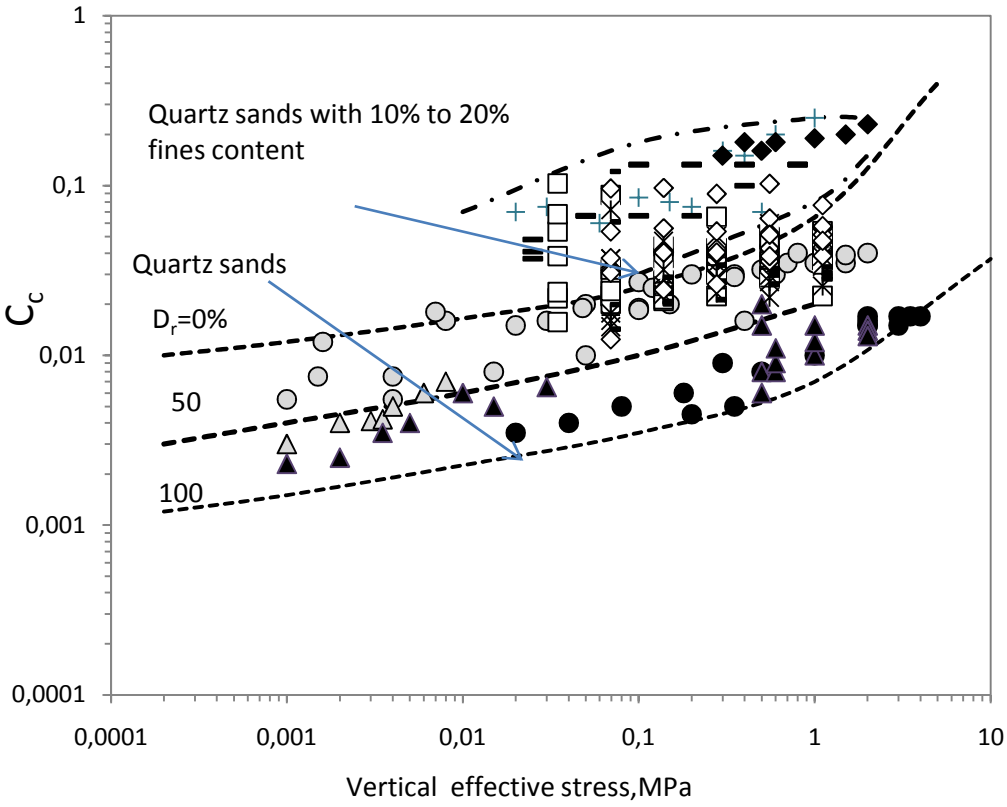

Data by Mesri and Vardhanabhuti (2009)

Particle shape	Quartz		Quartz with 10% to 20% fines content	
	loose	Dense	Loose	Dense
Well rounded to subrounded	○	●		
Angular to subangular	△	▲	+	◆

This study

Artificial silt RD=30%	Artificial silt RD=50%	Artificial silt RD=65%	Belgium silt RD=50%	Monkul al (2007)
□	-	✕	◇	-

Figure 7. 9 Data on C_c for different groups of sands (Modified from Mesri and Vardhanabhuti, 2009).

From Table 7. **5**, the compression index for loading steps of 140 kPa and 1108 kPa has values varying from 0.02-0.05 for mixtures A and 0.02-0.1 for mixtures B. These values show that the mixtures A have a low compressibility compared to that of the mixtures B.As one can see the values of compression index of artificial silt sandy measured are in same range as those reported for mine tailings (e.g. Aubertin et al, 1996).These results compared fairly well with those obtained on sandy soils as reported by Monkul et al (2007) that compression index is between 0.05 and 0.1 for sand with different fines contents. The C_c values for these soil mixtures are however much lower than those found in clayey silt mixtures such as Belgium silt samples which has compression index which varies between 0.02-0.1 which correspond to natural sandy silt with C_c equals to 0.16 as measures by Kaufman and Sherman(1964).

Table 7. 5 C_c values for different fines content and relative density

	Artificial silt						Belgium silt	
	RD=30%		RD=50%		RD=65%		RD=50 %	
FC,%	C_c , -		C_c ,-		C_c ,-		C_c ,-	
	140 kPa	1108 kPa	140 kPa	1108 kPa	140 kPa	1108 kPa	140 kPa	1108 kPa
7	0,04	0,05	-	-	0,03	0,04	0,05	0,05
10	0,02	0,04	0,03	0,03	0,02	0,03	0,04	0,06
15	0,03	0,05	0,03	0,04	0,02	0,03	0,02	0,04
20	0,03	0,04	0,03	0,03	0,05	0,04	0,04	0,05
25	0,02	0,04	0,03	0,04	0,02	0,03	0,04	0,05
30	0,02	0,02	0,02	0,03	0,05	0,06	0,06	0,06
50	0,04	0,04	0,02	0,03	0,02	0,03	0,10	0,08

From figure 7.10 and 7.11, the compression index of mixtures A decreases with increase of fines content from 7% to 10% and then it fluctuates for fines content between 15 and 25 % around a low value and remains low or increases slightly for higher fines contents.

In comparison, the compression index of mixtures B shows a clear trough for fines content between 10 and 25 %. For fines content above 25%, the compression index increases sharply with increasing fines content. Except at the deepest point of the trough, the mixtures B show more compressibility than the mixtures same relative density.

Figure 7. 10 and Figure 7. 11 shows that the compressibility decreases with an increase in relative density, as would be expected. For relative densities of 30% and 50% the compression index values are similar but lower than the values for a relative density of 65%, even though the difference is not large.

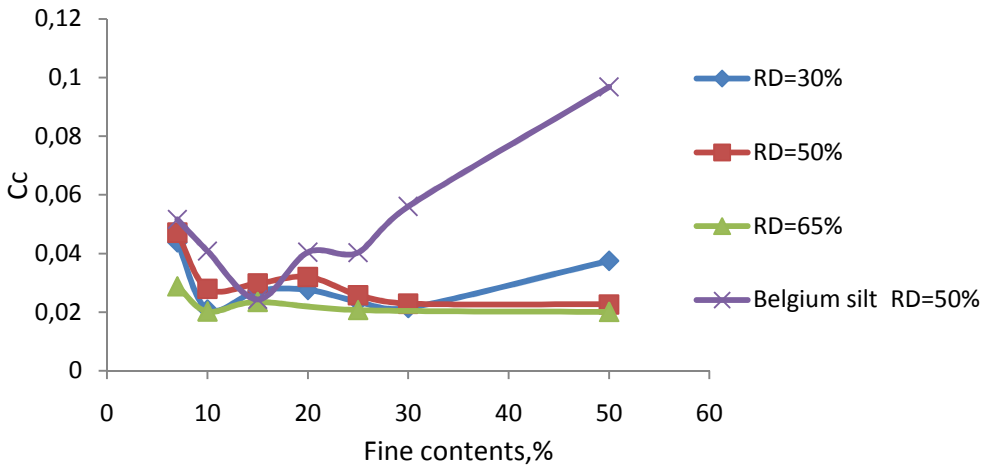

Figure 7. 10 Relationship between fines contents, compression index and relative density at 140 kPa

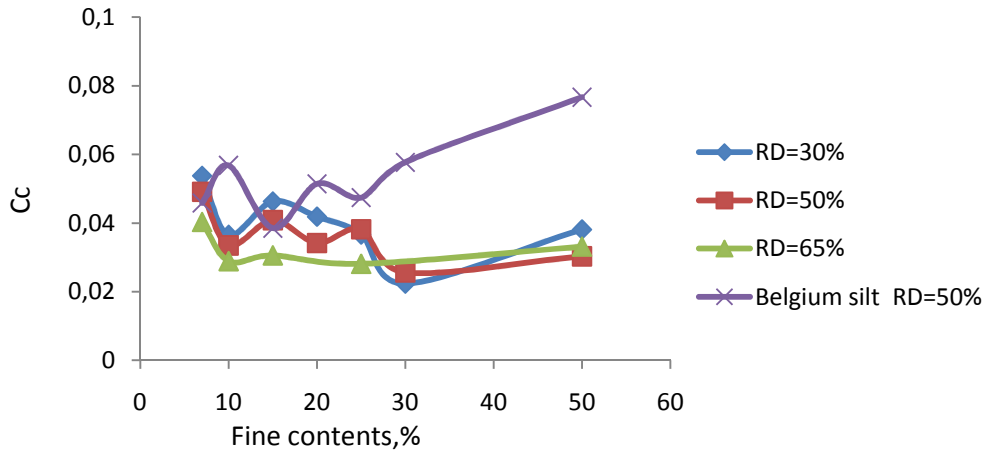

Figure 7. 11 Relationship between fines contents, compression index and relative density at vertical effective stress of 1108.3kPa

7.5 Modified coefficient of compression index

Modified coefficient of compression index is obtained from relationship between linear strain and stress .It can be described by equation 8.1 below

$$C_{\alpha\varepsilon} = \frac{\Delta \varepsilon_l}{\Delta \log \sigma_v'} \qquad (8.1)$$

Where $C_{c\varepsilon}$ is modified compression index, $\Delta\varepsilon_l$ is change in linear strain and $\Delta\log\sigma_v'$ is change in logarithmic of stress. Ladd (1971) pointed out that two samples may show very different void ration versus logarithm of effective stress plots but may have similar strain versus logarithmic effective stress curves because of the difference in initial void ratio.

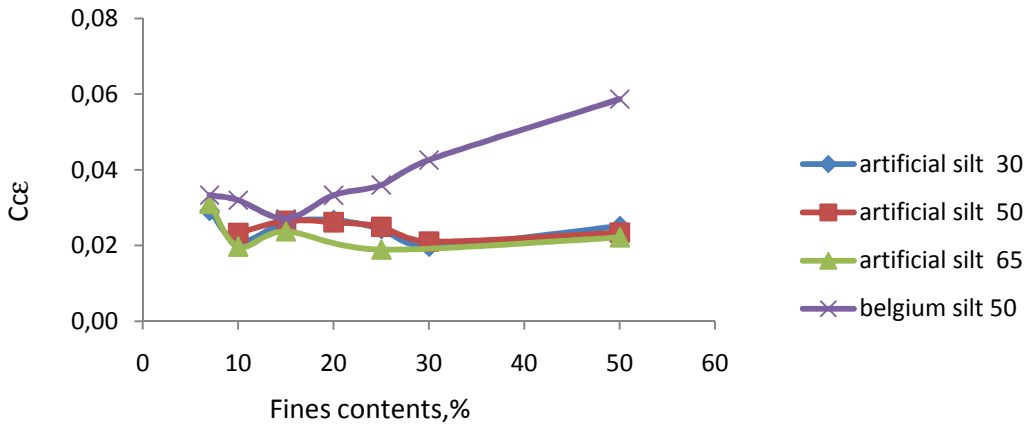

Figure 7. 12 Relationship between fines contents, modified compression index and relative density

Figure 7. 12 show relationship between modified compression index and fines content for mixtures. As one can see, the modified compression index for mixtures A decreases with increase of fines content from 7% to 10% and then it fluctuates for fines content between 15 and 25 % around a low value and remains low or increases slightly for higher fines contents. The influence of relative density is not seen, but the difference in mineralogy is highly pronounced as it can be seen from the figure 7.12. While for the modified compression index of mixtures B shows a clear trough for fines content between 10 and 25 %. For fines content above 25%, the compression index increases sharply with increasing fines content.

7.6 Intergranular void ratio concept

Intergranular void ratio concept employ the concept of using the void ratio created by the granular material and considers the fines as voids. Based on this concept the influence of fines on the compressibility of sand silt mixture can be depicted.

Figure 7.13, shows variation of intergranular void ratio with vertical effective stress. These curve have similar features as those plotted for vertical effective stress as function of void ratio. However, using intergranular void ratio the curves are shifted in position but the nature of deformation of the sample remain the same.

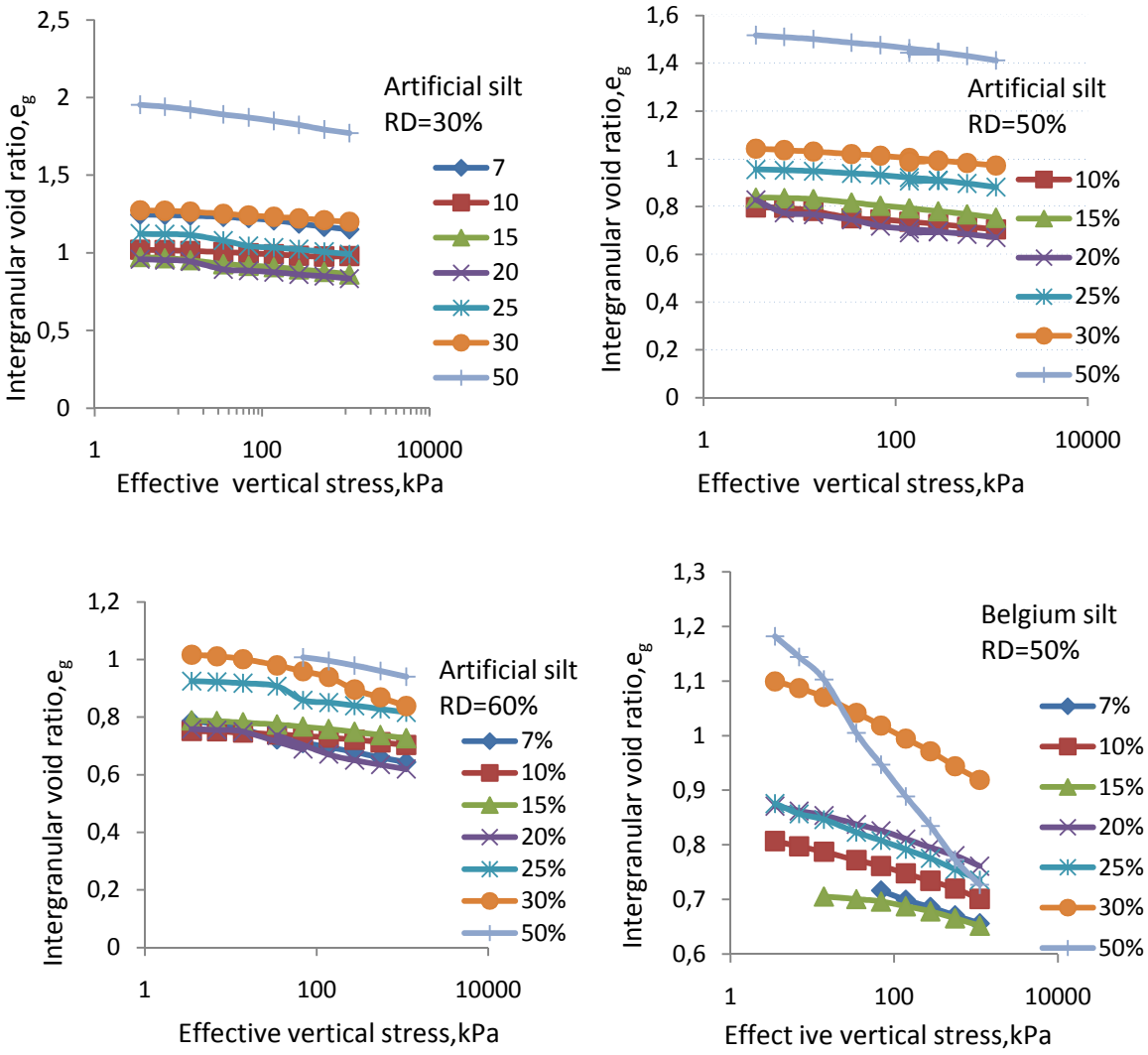

Figure 7. 13 Relationship between intergranular void ratio and effective vertical stress

Monkul and Ozden (2005) introduced the concept of transition fines content as fines content at which contact between grains occurs. In this concept, it is assumed that direct grains contacts of coarse grains can be initiated when intergranular void ratio of the mixture become equal to the maximum void ratio of the host granular material. Transition fines content is determined by intersection of maximum void ratio line with intergranular void ratio against effective vertical stress curves.

In this study, as it can be seen from figure 7.14, mixtures A with relative density of 30% have intersection between maximum void ratio line with intergranular void ratio between 33 to 35%,this indicates that the grain-grain contact for sand for applied

stresses is formed at fines content of 33 to 35%.For mixtures A with relative density of 50% the intersection is formed at fines content at 45% and for mixtures A with relative density of 65% and mixtures B no intersection is formed which indicates that the contact between coarse grains is established in low stresses. However for mixtures B the contact between grains are formed at low stress and it is expected that the mixtures will have low compressibility due to the fact that the contacts between grains increases the shear resistance , instead the mixture is more compressible than expected. This indicates that, there are other factors other than physical properties of sand and fines that influence the compressibility of sand silt mixtures.

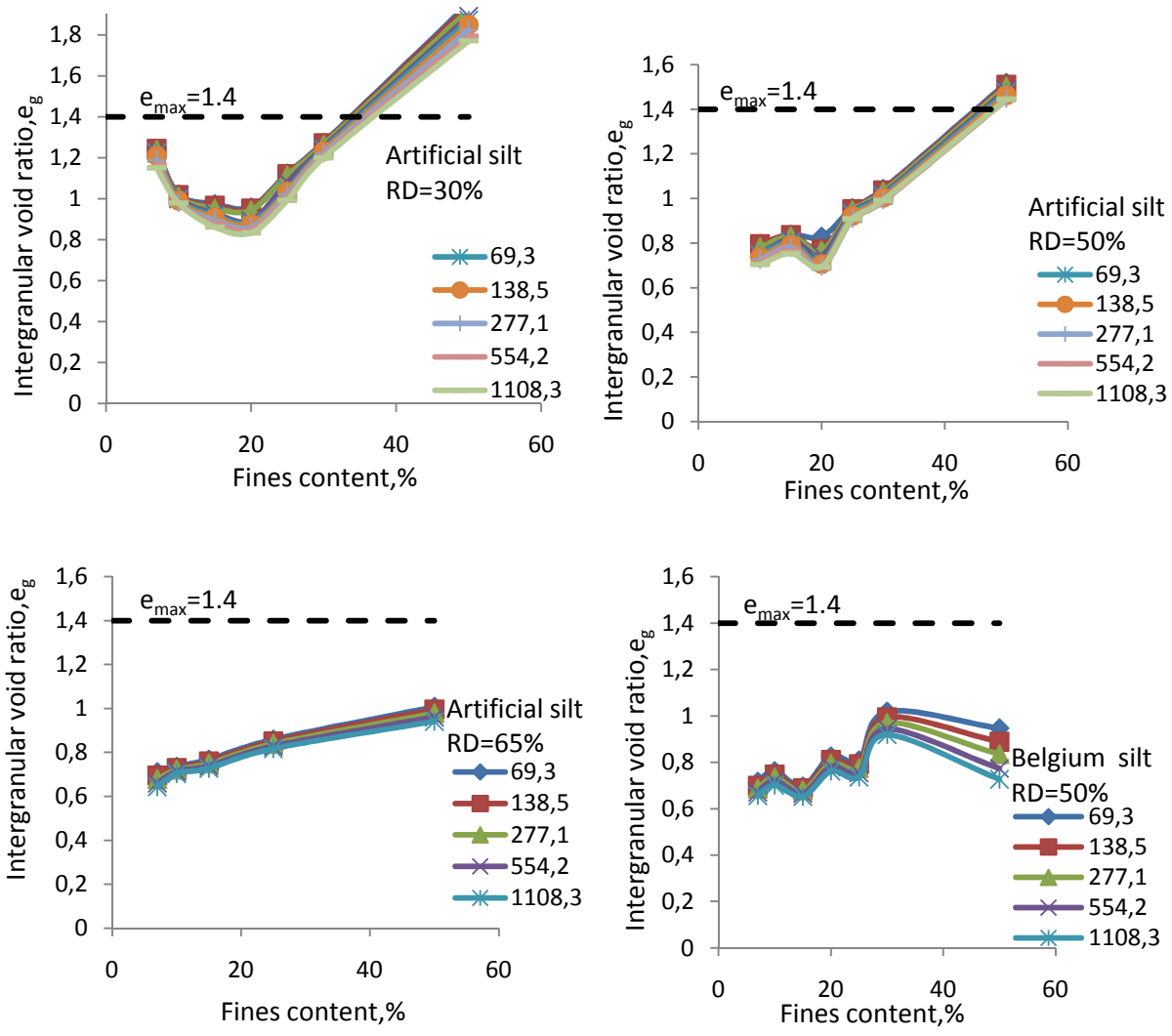

Figure 7. 14 Relationship between intergranular void ratio and fines content

7.7 Granular compression index (C_{c-s})

The granular compression index (C_{c-s}) was introduce by Monkul and Odzen ,2005. The importance of this parameter is on depicting the compressional characteristics of the silt sand mixture.

The definition of C_{c-s} is similar to the definition of compression index Cc and is expressed based on the decrease of intergranular void ratio with effective stress increment as in equation 7.1

$$C_{c-s} = \frac{\Delta e}{\Delta \log \sigma'} \qquad (7.1)$$

Figure 7.15 ,shows relationship between C_{c-s} and fines content.The trend observed in these curve is the same as those shown in the figure showing relationship between Cc and fines content.

Relationship between C_{c-s} and fines contents it shows clear the influnce of fines n compressibility as one can see from figure 7.15. Mixtures with fines content below 10% Cc-s decrease with increase fines content while for mixture between 10 and 25% have low C_{c-s} values while for mixture above 25% C_{c-s} values increases with and increase in fines content.

Tested material show to have low Cc-s compared to material tested by Monkul et al (2007) as it can be observed in the figure 7.15.This can be due to the difference in mineralogy and grain sizes in the mixtures.Relationship between Cc-s and fines contents doesn't shows clear differences in relative density at which the mixtures where tested but it interprete compression of material clearly.

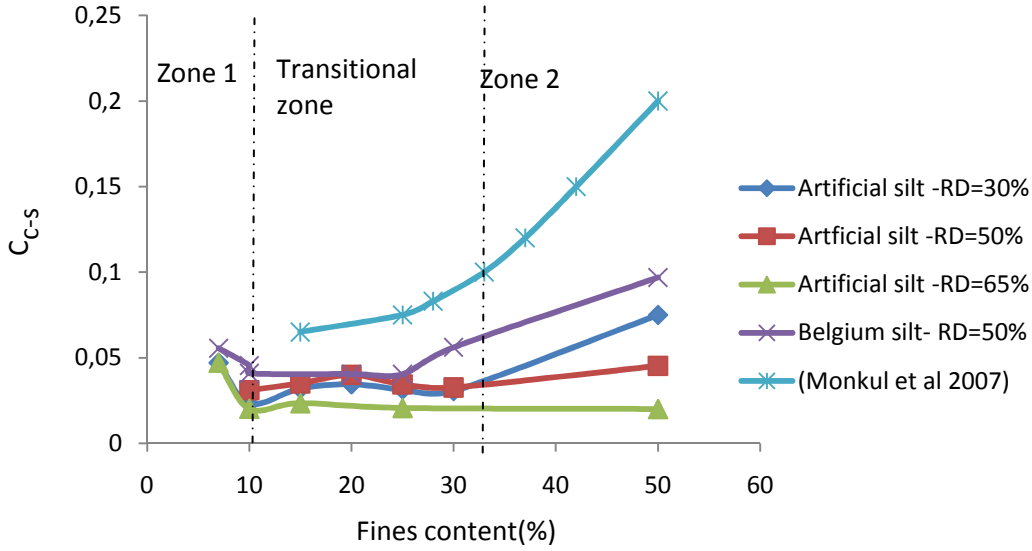

Figure 7. 15 Relationship between Cc-s and fines contents

As mentioned by Monkul et al (2007), figure 7.15 shows clearly the compression behavior of sand –silt mixtures. There are three zones can be observed in figure 7.15 (i.e. zone 1, transitional zone and zone 2).

In zone 1, the coarse grain matrix can be assumed to have almost a continuous framework with grain to grain contacts and fines are mostly located in the intergranular voids and in the contacts between the grains, as load applied the fines at the contacts tends to move and fill the intergranular voids, hence compressive behavior decrease with increase in fines contents in this zone. In transition zone, all fines available fill the intergranular voids and hence forming the continuous framework with grains to grain contact. In zone 2, as fines increases, sand grains become more dispersed so that there exist almost no grain contact and therefore the compressibility of the soil continues to increase and it is controlled by the finer grain matrix.

7.8 Summary

- Oedometer stiffness of the mixtures between 10 to 30% fines contents was expected to be high instead it is low due to its initial weak structure and high compressibility of the mixtures
- Mixtures with artificial silt (non plastic fines) coefficient of consolidation decreases with increase effective stress while for Belgium silt samples mixtures (with low plastic fines and platy material) the coefficient of consolidation increases with an increasing effective stress.
- The recompression index for all mixtures is high due to destructuring of the sample during initial loading.
- Compression index for mixtures depends on fines content in the mixture. For mixtures with fines content of 15-30%, the compression index is low compared to the mixtures with fines content below 15% and above 30%.
- Mineralogy of fines influences the compression index of the mixtures where mixtures with artificial silt have low compression index compared to the mixtures with Belgium silt which is natural silt have higher compression index .
- Intergranular void ratio concept is not suitable to define the transition fines content.
- Granular compression index is suitable to characterize the compressibility of the granular materials

Chapter 8

Data analysis and Interpretation - Secondary compression.

In this chapter discussion and analysis for secondary compression is done. Secondary compression is continuation of process after primary compression. In secondary compression only time is main factor for consideration.

8.1 Coefficient of secondary compression (C_α)

In this section the relationship between secondary compression and effective stress and fines contents is discussed.

Figure 8. 1 shows relationship between the coefficient of compression and the vertical effective stress. Results obtained for different relative densities and fines contents show that secondary compression varies with effective stress. However, a clear trend valid for all relative densities and fines contents cannot be seen.

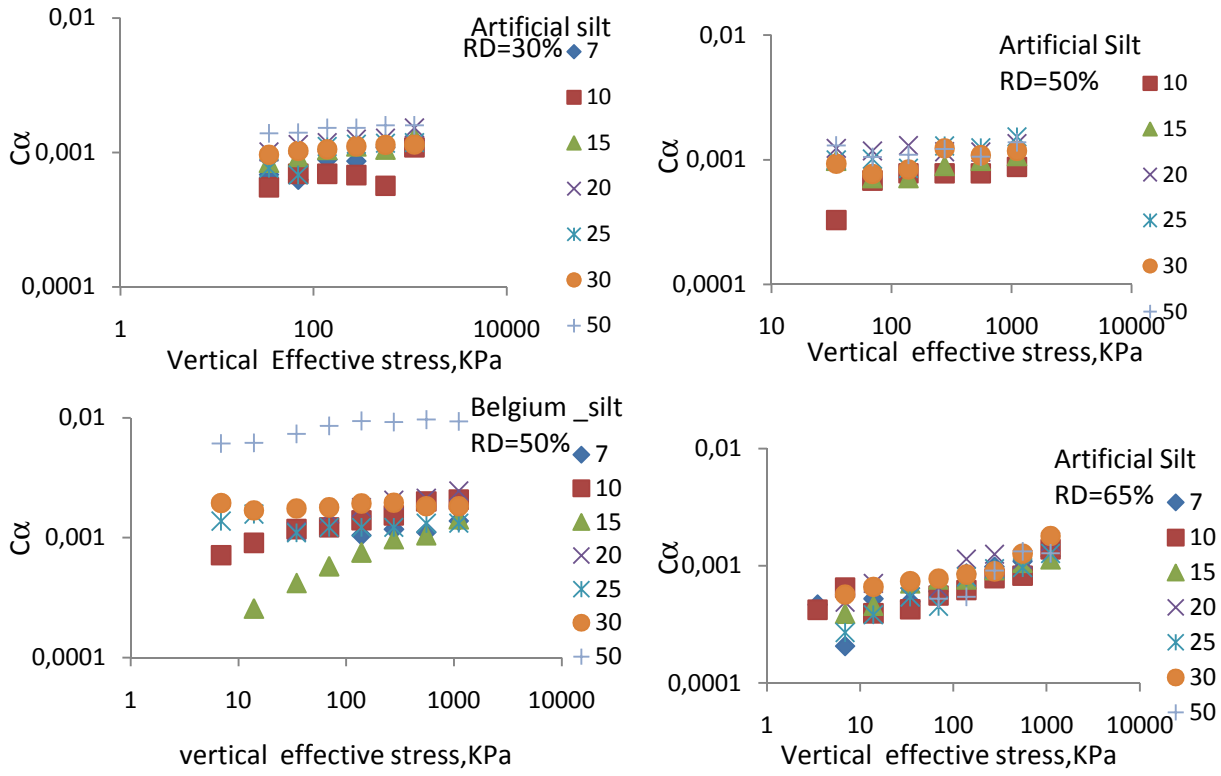

Figure 8. 1 Relationship between vertical effective stress and C□

In

Table 8. 2, the values of $\mathbf{C_\alpha}$ are given for vertical stress of 140 kPa and 1108 kPa. They range from 0.00075-0.001 for the mixtures A. This indicates that the secondary compression effect on these soils is very low. For the mixtures B, the values of $\mathbf{C_\alpha}$ varies from 0,001-0,002 which indicates that the influence of secondary compression on these soil is medium. This classification is based on secondary compressibility classification by Mesri (1973) as shown in table 8.1.

Al Shamrani (1998) reported C_α values for sabkha to be in the range of 0.0015 to 0.003 which correspond to the values obtained from this study of 0.00075 to 0.002.These values are quite comparable with the coefficient of secondary compression reported by various investigators for sandy soils(e.g. Leroueil and Marques (1996)).

Table 8. 1 Secondary compression classification by Mesri (1973)

C_α	Secondary compressibility
<0.002	very low
0.002–0.004	low
0.004–0.008	medium
0.008–0.016	high
0.016–0.032	very high

Table 8. 2 C_α Values for different fines content and relative density

	Artificial silt						Belgium silt	
FC,%	RD=30% C_α,–		RD=50% C_α,–		RD=65% C_α,–		RD=50% C_α,–	
	140 kPa	1108 kPa	140 kPa	1108 kPa	140 kPa	1108 kPa	140 kPa	1108 kPa
7	0,0009	0,0012	-	-	0,0009	0,0012	0,0010	0,0014
10	0,0007	0,0011	0,0008	0,0009	0,0006	0,0014	0,0014	0,0021
15	0,0010	0,0013	0,0007	0,0011	0,0008	0,0011	0,0008	0,0014
20	0,0012	0,0015	0,0008	0,0013	0,0011	0,0016	0,0013	0,0014
25	0,0011	0,0012	0,0009	0,0015	0,0008	0,0013	0,0012	0,0013
30	0,0011	0,0011	0,0008	0,0012	0,0008	0,0018	0,0019	0,0018
50	0,0015	0,0016	0,0011	0,0014	0,0008	0,0013	0,0019	0,0018

Figure 8. 2 and Figure 8. 3 shows the relationship between fines contents and secondary compression C_α for vertical effective stress of 140 and 1108 kPa**.** For the mixtures A, C_α fluctuates around a very low value whatever the fines contents and relative density are.

For the mixtures B, C_α increases slowly with increase of fines content up to 25%. At 30%, it jumps up significantly and decreases slightly to 50% fines content. It is only

at fines contents of 30% that the mixtures B exhibit more secondary compression than the mixtures A.

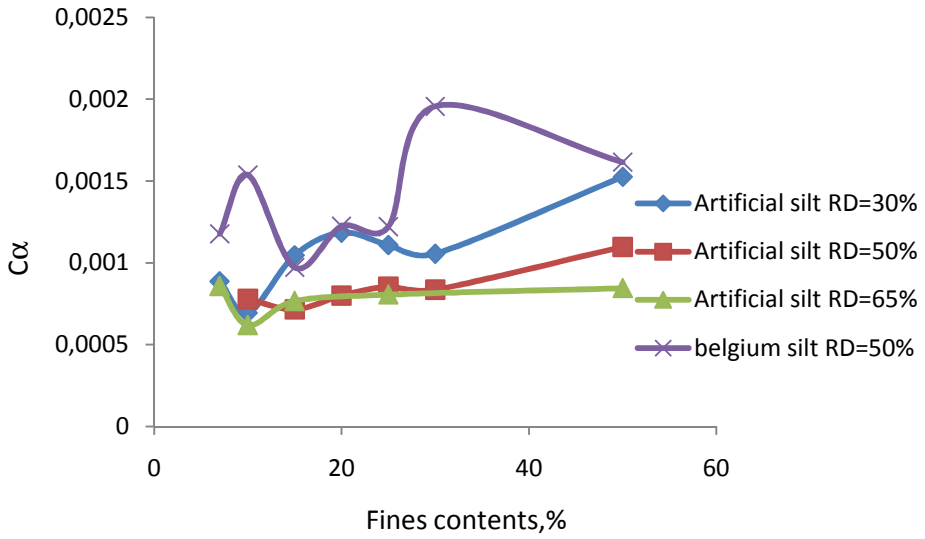

Figure 8. 2 Relationship between Coefficient of secondary compression and fines contents for the mixtures A and B at vertical effective stress of 140 kPa

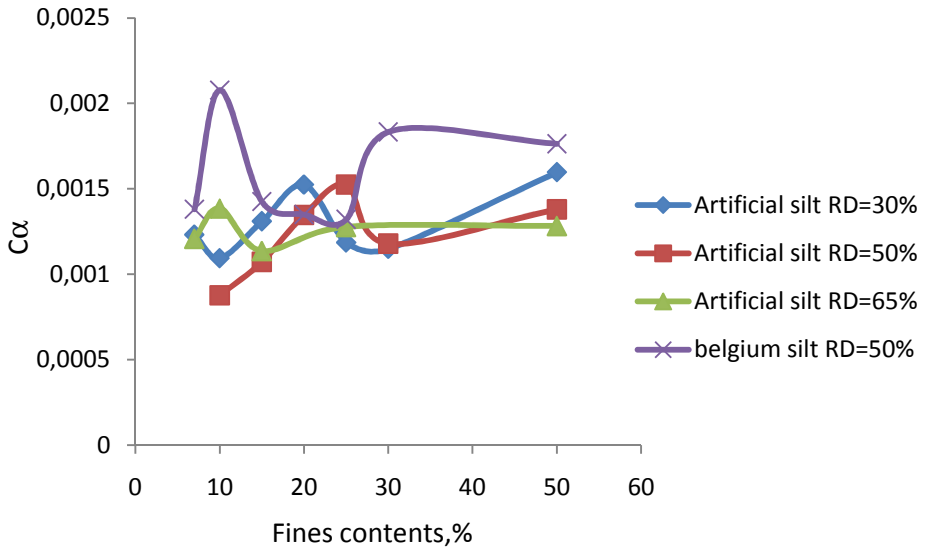

Figure 8. 3 Relationship between Coefficient of secondary compression and fines contents for the mixtures A and B at vertical effective stress of 1108 kPa

8.2 Modified coefficient of secondary compression.

Modified coefficient of secondary compression is obtained from relationship between linear strain and time .It can be described by equation 8.1 below

$$C_{\alpha\varepsilon} = \frac{\Delta\varepsilon_l}{\Delta \log t} \tag{8.1}$$

Where $C_{\alpha\varepsilon}$ is modified coefficient of secondary compression , $\Delta\varepsilon_l$ is change in linear strain and $\Delta \log t$ is change in logarithmic of time. Ladd (1971) pointed out that two samples may show very different void ration versus logarithm of effective stress plots but may have similar strain versus logarithmic effective stress curves because of the difference in initial void ratio.

Figure 8.4 shows relationship between modified coefficient of secondary compression and fines content for mixtures. As one can see the ,the variation of modified secondary compression is almost constant for fines content below 25% but the variation is considerable for fines content above 25%.Influence of relative density is not seen ,but the difference in mineralogy is highly pronounced as it can be seen from the figure 8.4.

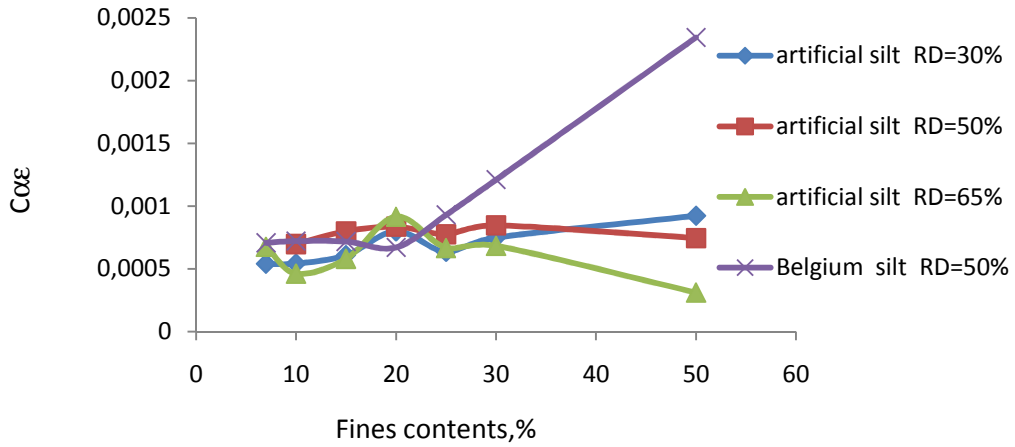

Figure 8. 4 Relationship between modified coefficient of secondary compression and fines contents for the mixtures A and B.

From the figure 8.4, it can be shown that the effect of mineralogy can be highly considered if the fines content is above 25%, but for mixtures with fines content below 25% the influence of fines on the secondary compression is minimal.

8.3 Cα/Cc relationship

Mesri and Godlewski (1977) studied the relationship between C_α and C_c, and concluded that volume changes during secondary compression and primary consolidation are caused by the same mechanisms. They proposed to study C_α/C_C for analysis of secondary settlement.

The use of the ratio C_α /C_C is based on the observation that magnitude and behaviour of C_α with time is directly related to magnitude and behaviour of C_C .

From the results obtained from the tests, a plot of corresponding values of C_α and C_C is shown in the Appendix C-4.The value of C_α was obtained from the linear part of the $e-\log t$ curve immediately after completion of primary consolidation and transition to secondary compression. The corresponding value of C_c for the same load increment was obtained from the EOP $e-\log \sigma'_v$ curve.

In the plot of C_α against C_c ,the regression line doesn't pass through the origin but instead have minimal positive intercept on the vertical axis. As suggested by Mesri and Castro (1987), the line of regression should pass through the origin. Fox et al (1992) and Al-Shamrani (1998) found that for peat and sabkha soils respectively, the fitting line do not pass through the origin. See appendix C-4.

The values for C_α / C_c for the tested soil samples are in the range of 0.017-0.04 as shown in the Table 8. 3. They are within the ranges reported for inorganic silt (0.03-0.05) and granular soils (0.015-0.03) according to Mesri and Vardhanabhuti, (2009). The values of C_α / C_c for most soils lie within the narrow range of 0.01 to 0.07, (Mesri and Castro, 1987).

Table 8. 3 C_α / C_c values for different fines contents and relative density

	Artificial silt			Belgium silt
FC,%	RD=30% $C_\square / C_c$	RD=50% $C_\square / C_c$	RD=65% $C_\square / C_c$	RD=50% $C_\square / C_c$
7	0,0166	-	0,0236	0,0294
10	0,0199	0,0168	0,0231	0,0387
15	0,0151	0,0260	0,0250	0,0344
20	0,0141	0,0383	0,0241	0,0352
25	0,0235	0,0327	0,0245	0,0291
30	0,0254	0,0375	0,0240	0,0295
50	0,0278	0,0395	0,0350	0,0445

Figure 8. 5 and Figure 8. 6 shows the ratio C_α / C_c for different fines contents. The values of C_α / C_c increases as fines contents increases. These values of C_α / C_c do not depend on the relative density of the sample, as it can be seen the values are almost the same for all relative densities. It was expected for Mixtures B

to behave clay like which is different from mixtures A. But the difference in mineralogy is not observed in the C_α/C_C relationships.

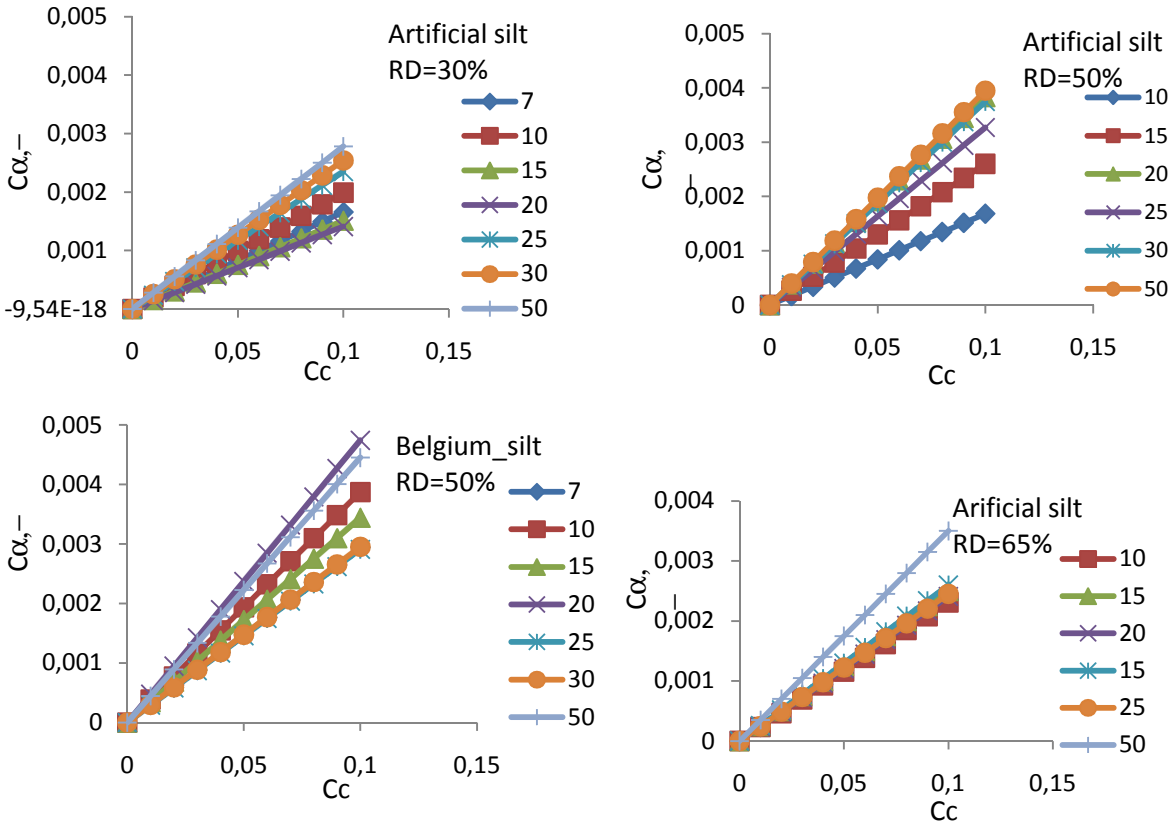

Figure 8. 5 C_α/C_c relationships for silt sand mixtures

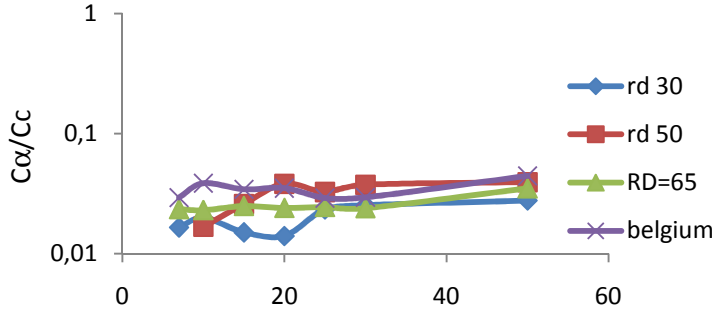

Figure 8. 6 Relationship between C_α/C_c and fines content

8.4 Summary

Based on analysed data, the following conclusion can be drawn regarding secondary compression of silt sand mixture tested,

- Mixture shows low secondary compression values
- According to Mesri classification on secondary compression ,silt sand mixtures are classifies as low secondary compression material
- Modified coefficient of secondary compression shows that for mixtures with fines content below 25% have low secondary compression while with fines content above 25% have high secondary compression , therefore the influence of fines is highly pronounced for mixtures with fines content above 25% and not below 25%.
- Relationship between C_α and C_c of silt sand mixtures is between inorganic silt and sand.
- There are no clear effects of fines content on the C_α /C_c, the values are constant but it is expected C_α /C_c to increase with fines contents.

Chapter 9

Laboratory results interpretation

In this chapter, the oedometer data presented in the former chapter is summarized, interpreted and discussed in taking into account the physical characteristics of the materials tested as well as the literature on the compressibility of sandy mixtures. Models of the initial soil fabric and their changes under vertical loading are proposed to as an interpretation tool to better understand the compressibility behavior of the silt sand mixtures.